ADDIS ABABA UNIVERSITY

ADDIS ABABA INSTITUTE OF TECHNOLOGY
SCHOOL OF MECHANICAL AND INDUSTRIAL ENGINEERING

AERODYNAMIC CHARACTERISTICS AND AERODYNAMIC SHAPE OPTIMIZATION OF ETHIOPIAN NATIONAL TRAIN, CASE STUDY ON ADDIS ABABA DIRE DAWA PASSENGER TRAIN

By

Mamo Nigusie

A Thesis Submitted to the School of Graduate Studies of Addis Ababa University in Partial Fulfillment of the Requirements for the Degree of Masters of Science in Mechanical Engineering (Railway Stream)

Advisors:-Dr.Ing Demiss Alemu

& Tsegaye Feleke

Addis Ababa University

October, 2014

ADDIS ABABA UNIVERSITY | DEPARTMENT OF MECHANICAL ENGINEERING

Addis Ababa Institute of Technology

School of Mechanical and Industrial Engineering

Aerodynamic Characteristics and Aerodynamic Shape Optimization of Ethiopian National Train, Case Study on Addis Ababa Dire Dawa Passenger Train

By

Mamo Nigusie

October, 2014

Approved by Board of Examiners:

Dr. Birhanu Beshah Head, Railway Centre	Signature	27/10/14 Date
Demiss Alemu (Dr.Ing.) Advisor	Signature	27/10/14 Date
Tsegaye Feleke Advisor	Signature	27/10/14 Date
Kamil Dino Internal Examiner	Signature	27/10/14 Date
Dr. Tesfaye Dama External Examiner	Signature	27/10/14 Date

Aerodynamic Characteristics and Aerodynamic Shape Optimization of Ethiopian National Train, Case Study on Addis Ababa Dire-Dawa Passenger Train, 2014

ABSTRACT

The aim of this study is to study and improve the aerodynamic performance (drag coefficient, lift coefficient, etc.), to reduce the energy consumption and checking the operational safety of the train against cross wind. The area of the study mainly concentrated on the frontal aerodynamic drag analysis and related characteristics of Ethiopian National Train (ENT).In particular Addis Ababa Dire Dawa 120 km/hr. speed passenger train is used for the analysis. The computational fluid dynamics (CFD) analysis simulation method is used for the study. To improve aerodynamic drag performance shape optimization of train head is done using multi-objective approximation integrated with computational fluid dynamics and response surface methodology. For the CFD full scale analysis ANSYS fluent 12.0 using steady RANS method is used. For the study of the stability against cross wind the wind with yaw angle -30 to 60 degree is analyzed. Results shows that the train has poor aerodynamic performance at this speed and shape which has around 0.93 drag coefficient. Also has poor performance against cross wind, hence care must be taken especially on the curves and embankment. After shape optimization drag coefficient of around 0.79 is obtained which is close to minimum recommended result (0.5).This result in reduction of more than 15% drag coefficient and this shows reduction in energy consumption.

Key words: *CFD, aerodynamic drag, shape optimization, cross wind stability,*

ACKNOWLEDGEMENT

During the course of my paper work, there were many people who were instrumental and morally helping me. Without their guidance, help and patience, I would have never been able to accomplish the work of this thesis. I would like to take this opportunity to acknowledge some of them.

Firstly I am grate full and would like to express my sincere gratitude to my supervisors Dr. Ing Demiss Alemu and AtoTsegaye Feleke for their appreciable ideas, invaluable guidance, continuous encouragement and constant support in making this thesis possible. In addition I would like to thank Dr.Idessa Diribsa for his ideas and support.

Secondly I would like to thank AAiT and all stuff of Department of Mechanical and Industrial Engineering because of their great support in completing the course and doing this thesis.

Next I would like to thank Ethiopian Railway Corporation (ERC) for their appreciable financial and technical support.

Lastly but not the least I would like to thank all of my friends and my family for their encouragement, and support with different materials and ideas.

TABLE OF CONTENT

Contents page

LIST OF TABLES

LIST OF FIGURES

NOMENCLATURE

A	Area
C_f	Coefficient of friction along wall
C_l	Coefficient of Lift
C_d	Coefficient of Drag
C_p	Coefficient of Pressure
D	Drag force
g	Gravity
$K-\varepsilon$	Turbulence model to simulate and read turbulent flow
M	Mach number
P	Pressure
Re	Reynolds number
Re_x	Reynolds number along a position x
U_{cl}	Centerline Velocity
u_∞	Fluid velocity
u	Friction velocity
U_{max}	Max. Velocity
V	Train Velocity
V_{inlet}	Inlet Velocity
y_p	Distance to the wall from center
y^+	Non-dimensionalized distance of first grid point from wall
ρ	Density

τ Shear Stress

μ Dynamic viscosity

$\dot{Q}_{net\ in}$ Rate of input energy

$\dot{W}_{net\ in}$ Rate input work

HST High Speed Train

RT Regional Type

ERC Ethiopian Railway Corporation

ENT Ethiopian National Train

AA-DD Addis Ababa-Dire Dawa

ETSC European Transport Safety Council

UIC International Union of Railways

CFD Computational Fluid Dynamics

LES Large Eddy Simulations

CAD Computer Aided Design

R Residual

N Number of iteration

F_x Aerodynamic drag

F_{px} Pressure Drag

$F_{\tau x}$ Friction drag

F_R Total drag

a, b, c Constants determined by the experiment

F_t Train velocity relative to the ground

q Dynamic pressure

s_x Cross-sectional area of the train

c_x Coefficient of aerodynamic drag

F_{xt} Drag of the leading car or locomotive

F_{xw} Drag of the tail car

F_{xz} Friction along the train

n Number of middle carriage

c_{xt} Drag coefficient of the leading car or locomotive

c_{xw} Drag of the tail car

c_{xz} Friction coefficient along the train

p_{bx} Skin pressure of the train along x axis

s_F Area of the train wall surface

τ_{ix} Shear stress on the train along x-axis

RANS Reynolds-Averaged Navier-Stokes

EIV Expected Improvement Value

MDO Multidisciplinary Optimization

RSA Response surface approximation

α Yaw angle

l_1 Length of upper curve

l_2 Length of the lower curve

c_1 Upper nose curve

h Height of the nose

c_2 Lower nose cure

dl_1 Change in length of upper curve

dl_2 Change in lower curve length

dh Change in nose height

DOE Design of experiment

FCCD Faced Centered Composite Design

$y_{c,new}$ Y-coordinate of the curve after the deformation,

$y_{c,old}$ Y-coordinate of the curve before deformation

i Coordinate point

n_c Number of coordinate points

L Length

H Height

W Width

CCD Center Composite Design

N Number of Design Variables

dy_{c1} Deformation coefficient c_1

dy_{c2} Deformation coefficient c_2

a Mechanical resistance

b Non-aerodynamic coefficient

b_1 Loss of quantity during the motion

b_2 Resistances caused by loss of gearing

c Aerodynamic drag term constant

k_w Relative velocity coefficient

k_y Change penetration coefficient

k_t Tunnel effect coefficient

r	Specific aerodynamic drag
i	Specific gradient resistance
r_c	Specific curve resistance
R	Total mechanical and aerodynamic drag
m	Train mass
c_x	Frontal aerodynamic coefficient
c_y	Lateral aerodynamic coefficient
c_p	Pressure coefficient
$\boldsymbol{F_x}$	The total effective force
ΔS	Change in distance
L_o	Mechanical labor
ū	Average fluid speed
F_o	Locomotive traction force
l_i	Indicated mechanical labor
η_1	Output/turnover of the locomotive
f_f	Friction factor
r_t	Specific mechanical drag of the locomotive

CHAPTER ONE: INTRODUCTION

1.1. History of Vehicle Aerodynamics: A General Background

Studies on aerodynamics have originated from aeronautics and marine applications. According to Barnard [2] at the turn of World War Two, substantial progress on aircraft aerodynamics was obtained due to the amount of research and analysis being done. Study of vehicle aerodynamics first began to surface during the earlier part of the 20th century and has continued up until the present day. During the earlier part of the 20th century, vehicle aerodynamics study is associated with vehicle performance. Aerodynamicists during that time carried out vehicle aerodynamics research with an aim to produce vehicles that can achieve a high speed to power ratio. To achieve high vehicle performance, much of the attention focuses on lowering the vehicle drag coefficient (Cd), which accounted to about 75 to 80% of total motion resistance at 100 km/h [2]. However, in the later part of the 20th century, during the oil crisis of 1973-1974, the focus on vehicle aerodynamics study shifted towards lowering the drag coefficient in order to produce vehicles with better fuel economy.

The trend shifted again in the early 1990's especially in North America where a low fuel price coupled with the increased popularity of light trucks and sport-utility vehicles have (of which drag coefficient of around 0.45), have reduced the importance the need on research to reduce drag coefficient [2]. Aerodynamicists then shifted their focus towards designing vehicle that provides maximum comfort to its occupants. Vehicle comfort consists of fine-tuning areas such as ventilation, heating, air conditioning and minimizing wind noise inside the vehicle.

1.2. Background on Train Aerodynamics

Among the different ways to travel such as airplane, car, bus or boat, the train is the safest. According to the report of the ETSC [7], between 2001/2002 the death per 100 million person kilometers is in the European Union 0.035 and the death per 100 million person hours is 2 which makes the rail the safest way to travel before ferry (respectively 0.25 and 8), aircraft (respectively 0.035 and 16) and bus (respectively 0.07 and 2). In addition, with the progress of technology, train is able to drive at high-speeds. On, the 3rd of April 2007 a TGV in France reached the velocity of 574.8 km/h. However this speed is only a record and the TGV trains drive generally between 200 and 330 km/h. The International Union of Railways (UIC)

defines that the speed of a high-speed train must be at least 200 km/h for upgraded track and 250 km/h for new track. For example, the TGV line between Paris and Strasbourg runs between 310 and 320 km/h.

With the increase of the train speed, aerodynamics has become an important key in the rail vehicles field. The study of the aerodynamics of a train can lead to substantial cost savings and more environmental friendly trains. The most studied phenomenon in the realization of a train is the drag generated by the displacement of the train in the air flow. Reducing the drag leads to a reduction of the amount of energy needed. But some others aerodynamic phenomena are of interests, such as the pressure variations while the train is driving in a tunnel, the study of the consequences of a crosswind, the study of the train rollover or the slipstream. A short overview of different aerodynamic phenomena is given below.

When a train runs, a strong head pressure pulse is created at the very front of the train which leads to a change of pressure in the surrounding. A low pressure bubble is also created at the rear part of the train but is less strong than the first one, and is mostly a problem for people or objects standing near to the track.

The pantograph is situated in an area where the flow conditions change a lot. In order to avoid unauthorized large variations of the contact surface it is important that the flow around the pantograph is not too turbulent, which can be enabled by adding some so called fairings.

While entering a tunnel the air at the train nose is compressed this creates an overpressure wave that migrates at the speed of sound. When this wave reaches the end of the tunnel a part of the wave is reflected and goes back as an under-pressure wave. As the train tail enters the tunnel an under pressure wave is created and migrates to the end of the tunnel. The pressure variation is maximum when an under pressure wave meets a reflected overpressure wave. The pressure difference reaches then a peak value. This mostly causes discomfort for the passenger since he is subject to a high pressure difference in a short time, for example the legislation in Sweden is 1500 Pa in 4 seconds [3].

The bogies movement is restricted to the tracks. A suspension system connects the train body to the bogies. The trains can then roll, yaw and pitch. A yawing moment can increase in strong crosswinds. This can be very dangerous in case of strong crosswind and particular yaw angle and can lead to overturning.

Aerodynamic noise comes from the pressure fluctuations that occur in the turbulent boundary layer and as the flow separates. Vortices produce also a lot of aerodynamic noise (von Karman vortex during flow separation). It is therefore important to have attached flow since the separation of the boundary layer creates a lot of noise. One can say that the power of external aerodynamic noise grows with about the sixth power.

As discussed above train travel is an efficient transportation alternative in comparison to other ways of transportation, but the increasing demand for energy efficiency calls for improvement. Much energy is lost when overcoming the air drag, and since the drag has a greater impact at higher speeds more research has been performed to reduce the air drag on high-speed trains than on low-speed trains. The high-speed trains therefore usually have a streamlined design, but the regional and freight-trains used in today are relatively old type and do not have an appropriate aerodynamic design.

By making small changes in the train geometry a large drag reduction could be achieved. Accurate descriptions of instantaneous flow around vehicles are important to fully understand what causes the air drag.

The drag arises both from friction on the surface of the vehicle and from the pressure difference between the front and the wake behind the vehicle. The instantaneous flow and what contributes most to the air drag can be examined by using Computational Fluid Dynamics (CFD).

For bluff bodies, such as trains, the method Large Eddy Simulations (LES) has proven to be a method that gives good results [4]. When improving the energy efficiency of vehicles, the lowering of the aerodynamic drag is an important aspect. Drag reduction on freight-trains could lead to both environmental and economic benefits as the energy consumption is lowered. Since not much research has been done on these types of trains it is of great interest to conduct CFD analyses to make them more energy efficient.

In this study it’s been tried to study the aerodynamic characteristics and aerodynamic shape optimization. Stability against cross wind and fuel economy is also analyzed.

1.3. Motivations and Previous Research

External aerodynamics is becoming an important field of study in recent years [5].This is because of its effectiveness in the study of visibility, comfort, stability, cooling and performance. In this study we consider the stability and flow performance around a train.

There is not much research performed on transient flow around vehicles, much depending on that the complex geometries of these make it difficult to perform both experimental and numerical studies.

Therefore simplified models of vehicles are often used for investigations of the drag. Most of the studies conducted on trains have often concerned high-speed trains and effects as compression waves and side winds. Few studies regarding drag reduction have been conducted on freight and regional-trains and most of those done are experimental.

Relevant research has been conducted regarding simplified bus-shapes which possess great similarities with a simplified train-shape. Wind tunnel tests performed on a simplified bus-shape found that the drag coefficient could be reduced remarkably by increasing the radii of the bus's corners and incorporating a vortex cavity trapper in the tail. There are also several studies made on cargo-wagons. Different geometries for cargo wagon tops have been tested and the tests showed that a bow shaped top perpendicular to the direction of travel of the train gave lower drag than a simple box shape. Other cargo-wagon studies concluded that it is preferable to cover the wagons instead of having open wagons and that the drag is significantly lowered if the sides of the wagon are smoothed.

Experimental studies have also been carried out on rectangular shapes, which had rounded edges at the front to resemble car geometries. Measurements were made on clean boxes with the same length and frontal area but with variation in aspect ratio (height divided by width). The result received was that the drag coefficients were found to increase when the aspect ratio was increased.

An experiment performed by Yutaka Sakuma and Atsushi Ido[4] tested different front-end shapes on rectangular boxes and the conclusion was that the drag could be lowered up to 50% if the edges were rounded or elliptic.

1.4. CFD, Theory and Governing Equations

1.4.1. CFD

Computational Fluid Dynamics or CFD is the analysis of systems involving fluid flow, heat transfer and associated phenomena's such as chemical reactions by means of computer based simulation [6].

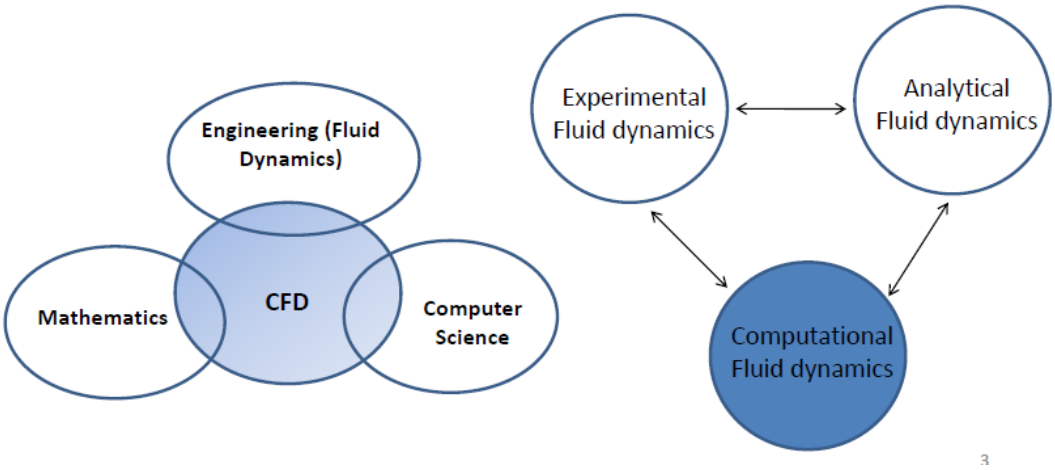

Figure1.1: CFD

The following section explains concepts, equations and models used in this thesis.

One of the biggest challenges in the engineering industry is being able to come up with efficient and optimal designs for new products. One of the strongest tools offered is FLUENT. FLUENT is a very useful program recently acquired by ANSYS. It has the capability to model fluid flow past objects with the ability to design, test, and analyze results all under one program [7, 9].

1.4.2. Theory and Governing Equation

ANSYS FLUENT is Computational Fluid Dynamics (CFD) software that allows users to simulate flow problems of ranging complexity. It contains broad physical modeling capabilities needed to model flow, turbulence, heat transfer, and reactions over objects designed by the user. Thousands of companies around the world benefit from the use of CFD software as a main part of their design phases in their product development. It uses the finite-volume method to solve the governing Navier-Stokes equations for a fluid which are derived from the conservation mass equation (1), the conservation of momentum (2) and the conservation of energy (3) equations [7, 9, 10].

The difficulty arises from the fact that the conservation of mass, momentum and energy are coupled and non-linear set of differential equations making them practically impossible to solve analytically for practical engineering problems. Hence CFD software such as FLUENT is utilized to provide very reasonable approximation upon solving the specified governing equations [7, 10].

Additionally, FLUENT also allows the users to model a range of flows such as incompressible or compressible, inviscid or viscous, laminar or turbulent flow. The advanced solver technology that FLUENT has, provides fast and accurate results through flexible moving and deforming meshes to be able to create optimal designs. Ultimately, FLUENT allows engineers to design, create and analyze a configuration all under one program.

In order to model the object that a user wants to work with, its geometry and mesh must be first created in ANSYS Workbench. Another option is to import the geometry and mesh from Computer Aided Design (CAD) software packages such as Unigraphics, ProE or others. In Workbench, the user creates the object he or she wishes to analyze and Workbench guides the user through very complex metaphysics for fluid flow with drag and drop simplicity. Once the geometry has been created, the user can take advantage of several meshing options that Workbench provides. The user can implement the meshing in the specimen to analyze the structure as they try to analyze fluid flow past/through their object.

The conservation mass equation:

$$\frac{\partial \rho}{\partial t} + \nabla \cdot (\rho \vec{V}) = 0 \quad \ldots 1$$

The conservation of momentum equation:

$$\rho \frac{\partial \vec{V}}{\partial t} + \rho(\vec{V} \cdot \nabla)\vec{V} = -\nabla \rho + \rho \vec{g} + \nabla \cdot \tau_{ij} \quad \ldots 2$$

The conservation of energy equation:

$$\frac{\partial}{\partial t}\int e * \rho \, d\forall + \int (\breve{u} + \frac{p}{\rho} + \frac{V^2}{2} + gz)\rho \boldsymbol{V} \cdot \breve{\boldsymbol{n}} \mathrm{dA} = \dot{Q}_{net\, in} + \dot{W}_{net\, in} \quad \ldots 3$$

A few different ways of modeling and analyzing fluid flow are through turbulence modeling, k-ε, and y^+. Turbulence modeling is used to model turbulent flow. Turbulent flows are characterized by large, nearly random fluctuations in velocity and pressure in both space and

time. These fluctuations arise from instabilities that eventually are dissipated (into heat) by the action of viscosity. Turbulent flows occur in the opposite limit of high Reynolds numbers. The two approaches to solving the flow equations for turbulent flow field can be roughly divided into two classes, direct numerical simulations and k-ε [7]. Direct numerical simulation numerically integrates the Navier-Stokes equations, resolving all of the spatial and temporal fluctuations without resorting to modeling. k-ε, models Reynolds stress in two turbulent parameters, the turbulent kinetic energy (k) and the turbulent energy dissipation rate ∈ defined below by Equations 4 and 5 respectively.

$$\kappa \equiv \frac{1}{2}\left(\overline{u'^2} + \overline{v'^2} + \overline{w'^2}\right) \dots\dots\dots\dots\dots\dots\dots\dots\dots\dots\dots\dots\dots\dots\dots\dots\dots\dots\dots\dots\dots\dots\dots\dots\dots\dots\dots\dots\dots\dots 4$$

$$\epsilon \equiv \upsilon[\left(\frac{\partial u'}{\partial x}\right)^2 + \left(\frac{\partial u'}{\partial y}\right)^2 + \left(\frac{\partial u'}{\partial z}\right)^2 + \left(\frac{\partial v'}{\partial x}\right)^2 + \left(\frac{\partial v'}{\partial y}\right)^2 + \left(\frac{\partial v'}{\partial z}\right)^2 + \left(\frac{\partial w'}{\partial x}\right)^2 + \left(\frac{\partial w'}{\partial y}\right)^2 + \left(\frac{\partial w'}{\partial z}\right)^2 \dots\dots\dots\dots\dots\dots\dots\dots\dots\dots\dots\dots\dots\dots\dots\dots\dots\dots\dots\dots\dots\dots\dots\dots\dots\dots\dots\dots\dots\dots 5$$

The next type of modeling is known as y^+. $y^+$is a mesh-dependent dimensionless distance that quantifies to what degree the wall layer is resolved. $y^+$is a non-dimensional parameter defined by Equation:

$$y^+ = \frac{\rho u y_p}{\mu} \dots\dots\dots\dots\dots\dots\dots\dots\dots\dots\dots\dots\dots\dots\dots\dots\dots\dots\dots\dots\dots\dots\dots\dots\dots\dots\dots\dots\dots\dots 6$$

Where u= $\sqrt{\frac{\tau_w}{\rho_w}}$ which is the friction velocity and y_p is the distance to the wall.

Workbench offers several meshing options, one being structured meshing. In structured meshing the user decides how many user defined shapes they want placed over the object they are analyzing. Structured meshing consists of tetrahedrons and exhibits a clearly pronounced pattern.

As the geometries increase in complexity it is necessary to adjust the meshing accordingly. However, when dealing with other cases such as flow across an airfoil, it is important to use a different mesh structure. One such structure is a structured "O- grid" around the airfoil. Because of the existence of the layers around the airfoil, it can be ensured the flow gradients are properly captured.

FLUENT obtains a solution such that the mass, momentum, energy and other quantities are conserved for each cell.

The code of the CFD software solves directly the values of the flow variables at the cell centers and the values at other locations are appropriately interpolated [7].In other cases, where there is no complicated geometry, but rather there is more flow gradients occurring around a certain area, the user can apply a bias.

Once the test object has been drawn and meshed in Workbench or imported from other software package (CatiaV5 for this paper case), FLUENT then allows the user to analyze it in different flow parameters. Another modeling capability FLUENT is capable of using is enhanced wall treatment. When the user chooses to use enhanced wall treatment, they can use this especially for turbulent cases using the k-epsilon model because it analyzes the object closer near the wall region.

The initial and boundary conditions can be specified in FLUENT and upon initializing the problem; it can be checked for convergence. If the convergence is not achieved accurate results will not be obtained. Finally, FLUENT provides a wide variety of parameters that can be plotted and analyzed.

In FLUENT during the obtainment of convergence the governing equations are solved for a predetermined by the user number of times (iterations). Specifically the magnitude of the average of particulate variable is computed as illustrated in Equation:

$$R = \sqrt{\frac{\sum_{i=1}^{N}(u_i - u_{gi})^2}{N}} \ldots\ldots\ldots\ldots\ldots\ldots\ldots\ldots\ldots\ldots\ldots\ldots 7$$

Where R is the residual, N is the number of iterations to be performed, u indicates a particulate variable to be computed, and the subscript g indicates a guessed value

The incompressible Navier-Stokes equations in Cartesian coordinates are shown in Equations below.

X-direction:

$$\rho\left(\frac{\partial u}{\partial t} + u\frac{\partial u}{\partial x} + v\frac{\partial u}{\partial y} + w\frac{\partial u}{\partial z}\right) = -\frac{\partial p}{\partial x} + \rho g_x + \mu\left(\frac{\partial^2 u}{\partial x^2} + \frac{\partial^2 u}{\partial y^2} + \frac{\partial^2 u}{\partial z^2}\right) \ldots\ldots\ldots\ldots .8$$

Y-direction:

$$\rho\left(\frac{\partial v}{\partial t}+u\frac{\partial v}{\partial x}+v\frac{\partial v}{\partial y}+w\frac{\partial v}{\partial z}\right)=-\frac{\partial p}{\partial y}+\rho g_y+\mu\left(\frac{\partial^2 v}{\partial x^2}+\frac{\partial^2 v}{\partial y^2}+\frac{\partial^2 v}{\partial z^2}\right) \ldots\ldots\ldots\ldots\ldots 9$$

Z-direction:

$$\rho\left(\frac{\partial w}{\partial t}+u\frac{\partial w}{\partial x}+v\frac{\partial w}{\partial y}+w\frac{\partial w}{\partial z}\right)=-\frac{\partial p}{\partial z}+\rho g_z+\mu\left(\frac{\partial^2 w}{\partial x^2}+\frac{\partial^2 w}{\partial y^2}+\frac{\partial^2 w}{\partial z^2}\right) \ldots\ldots\ldots\ldots 10$$

Drag and lift

The Drag Force, D, acts in the direction of the free stream while the Lift Force, L, is normal to the free stream. Objects such as airfoils are designed to generate lift. However for objects such as cars, trains, it is desired to reduce the lift since the lift on a car or train reduces the contact force between the wheels and the ground or rails. Typically the lift and drag are given in terms of the Coefficient of Lift and the Coefficient of Drag which are dimensionless forms of the Lift and Drag forces [7, 11, 12].

$$C_L=\frac{L}{0.5*\rho*U^2*A} \ldots\ldots\ldots\ldots\ldots\ldots\ldots\ldots\ldots\ldots\ldots\ldots\ldots\ldots\ldots\ldots\ldots\ldots\ldots\ldots\ldots\ldots\ldots\ldots\ldots\ldots 11$$

$$C_D=\frac{D}{0.5*\rho*U^2*A} \ldots\ldots\ldots\ldots\ldots\ldots\ldots\ldots\ldots\ldots\ldots\ldots\ldots\ldots\ldots\ldots\ldots\ldots\ldots\ldots\ldots\ldots\ldots\ldots\ldots\ldots 12$$

Fluid dynamics: Fluid dynamics is the study of the motion of fluids and the forces acting on the fluids.

1.4.2.1. Formation Mechanism of Train Aerodynamic Drag

In the open air condition, the aerodynamic drag of the train is the sum of the tangential forces (skin friction drag) and the normal forces (pressure drag), both of which are parallel to the opposition direction of vehicle's velocity vector [13, 14]. The pressure drag comes from the integral of the skin pressure of the train. The direction of drag is along the positive direction of x axis, as shown in Figure 1.2 below. The friction drag can be obtained by the integral of the tangential forces. The drag formula for the train in the open can be expressed as:

$$F_x = F_{px} + F_{\tau x} \ldots\ldots\ldots\ldots\ldots\ldots\ldots\ldots\ldots\ldots\ldots\ldots\ldots\ldots\ldots\ldots\ldots\ldots\ldots\ldots\ldots\ldots\ldots\ldots\ldots\ldots 13$$

Where F_x is the aerodynamic drag, F_{px} is the pressure drag and $F_{\tau x}$ is the friction drag.

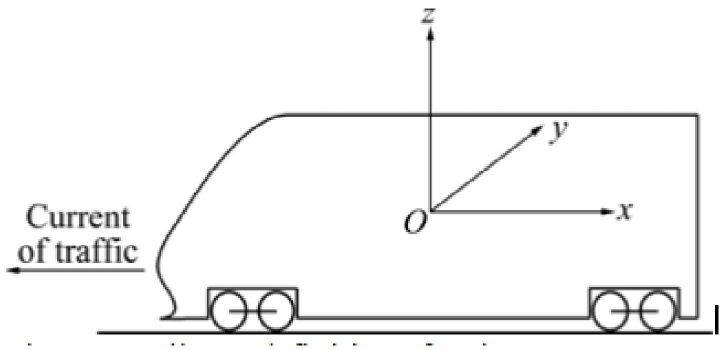

Figure1.2: Coordinate Definition of Train [13]

Therefore, the aerodynamic drag on the traveling train is divided into pressure drag and friction drag. The formation mechanism of the aerodynamic drag will be discussed in the following part.

1.4.2.2. Composition of Aerodynamic Drag

The train drag is divided into the aerodynamic drag, the sliding force between the wheel and rails, and the friction force caused by the pantograph system. The total drag of train was composed of the sum of each carriage drag.

1.4.2.3. Relationship between Aerodynamic Drag and Total Drag of Train

In the open air condition without any cross-wind effect, the total drag on the traveling train can be expressed by Davis experience formula [13]:

$$F_R = a + bv_t + cv_t^2 \quad \ldots \ldots \ldots \ldots \ldots \ldots \ldots 14$$

Where F_R is the total drag, a, b and c are the constants determined by the experiment, and v_t is the train velocity relative to the ground.

In general, in Eqn. 14 (above), the total drag can be divided into two contributions: $a + bv_t$ is the mechanical drag which includes the sliding drag between rails and train wheels, and the rotating drag of the wheels; and cv_t^2 is the aerodynamic drag. So the aerodynamic drag can be expressed as:

$$F_x = cv_t^2 \quad \ldots \ldots \ldots \ldots \ldots \ldots \ldots 15$$

The coefficient of aerodynamic drag (c_x) can be described as:

$$c_x = \frac{F_x}{qs_x} \quad \ldots \ldots \ldots \ldots \ldots \ldots \ldots 16$$

Where q is the dynamic pressure, and s_x is the cross-sectional area of the train.

Therefore, the aerodynamic drag can be written as

$$F_x = q s_x c_x = ½ \rho s_x c_x {v_t}^2 \quad \ldots\ldots\ldots\ldots\ldots\ldots\ldots\ldots\ldots\ldots\ldots\ldots\ldots\ldots\ldots\ldots\ldots\ldots\ldots\ldots 17$$

Compared with Eqns.(15) and (16), the coefficient (c)can be expressed as:

$$c = \frac{1}{2} \rho s_x c_x \quad \ldots\ldots\ldots\ldots\ldots\ldots\ldots\ldots\ldots\ldots\ldots\ldots\ldots\ldots\ldots\ldots\ldots\ldots\ldots\ldots\ldots\ldots\ldots\ldots 18$$

The aerodynamic drag is proportional to the square of speed of the strain, while the mechanical drag is proportional to the speed of the train. Compared with the mechanical drag, the portion of the aerodynamic drag becomes larger as the train speed increases.

1.4.2.4. Relationship between Aerodynamic Drag and Each Carriage Drag of Train

The aerodynamic drag of the train is composed of the drag of each carriage. The drag force can be written as:

$$F_x = F_{xt} + \sum_{i=1}^{n} F_{xz}(\mathrm{i}) + F_{xw} \quad \ldots\ldots\ldots\ldots\ldots\ldots\ldots\ldots\ldots\ldots\ldots\ldots\ldots\ldots\ldots\ldots\ldots\ldots\ldots\ldots 19$$

Where$F_x$is the total aerodynamic drag; F_{xt} is the drag of the leading car or locomotive; F_{xw} is the drag of the tail car; F_{xz}(i) is the friction along the train, which includes the bogies, wheels, interference, and bottom structure of the train; and n is the number of middle carriages. The coefficient (c_x) can be written as:

$$c_x = c_{xt} + \sum_{i=1}^{n} c_{xz}(\mathrm{i}) + c_{xw} \quad \ldots\ldots\ldots\ldots\ldots\ldots\ldots\ldots\ldots\ldots\ldots\ldots\ldots\ldots\ldots\ldots\ldots\ldots\ldots\ldots\ldots 20$$

Where c_{xt} is the drag coefficient of the leading car or locomotive; c_{xw} is the drag of the tail car; and c_{xz}(i) is the friction coefficient along the train, respectively.

1.4.2.5. Formation Mechanism of Pressure Drag

When the train runs at high speed, there will be a stagnation region with high pressure on the windward face of the train nose, and the flow speed will decrease. At the same time, the flow

moves at high velocity along the tail car and the pressure decreases. The pressure drag stems from the pressures due to the abrupt change in the cross-sectional area of the train. The pressure drag can be obtained by integrating along the whole car

$$F_{px} = \oint_{SF} p_{bx} d\, s_F \quad \ldots\ldots\ldots\ldots\ldots\ldots\ldots\ldots\ldots\ldots 21$$

Where,$p_{bx}$is the skin pressure of the train along x axis, and s_F is the area of the train wall surface`.

For the train, the pressure drag comes from the pressure due to the shape of fore-body and after-body of the train, the connecting parts between trains, the train wall surfaces, the pantograph system, the bogie, and underneath structure of the train. The mechanism of forming pressure drag is given as follows: there is a stagnation region in the leading car nose and air guide sleeve. The flow velocity of air is almost equal to zero, when the pressure reaches the largest in these regions. The flow around the pantograph system and bogie can also cause the increase of the skin pressure and the decrease of speed. And there are large pressure changes in the connecting parts between trains. When the air flow along the train reaches the end car, the flow speed will increase and the pressure will decrease. Air flow separation occurs at the nose of the end car. This results in a great change in the pressure distribution at the end car, leading to the pressure drag.

1.4.2.6. Formation Mechanism of Friction Drag

Due to the viscosity of the air, boundary layer occurs on the wall of train when the air flows along the train surface [13]. The height of boundary layer is equal to zero at the nose of the train, and becomes larger at the leeward. The speed of flow increases from zero to running velocity of the train along the boundary layer normal direction. The tangential forces are caused by the difference of the velocity in the boundary layer normal direction, which is shear stress on the train surface. Friction drag of the train is the sum of shear stress, which is in the reverse direction of the train running direction. Friction drag can be obtained by integrating along the whole train:

$$F_{\tau x} = \oint_{SF} \tau_{ix} ds_F \quad \ldots\ldots\ldots\ldots\ldots\ldots\ldots\ldots\ldots\ldots 22$$

Where,τ_{ix} is the shear stress on the train along x-axis

The shear stress is proportional to the viscosity of the air (μ) and the velocity gradient. The velocity is related to the height of boundary layer. However, the boundary is closely related to the shape of the train, the smooth of the train wall, the running velocity and the ambient surround. Therefore, the friction drag is relevant to the shape of the train, the smooth of train surface, the running velocity and the ambient surround.

1.4.2.7. Measures of Reduction of Aerodynamic Drag

When the train runs at high speed, the flow around the train will be formed due to the viscosity of air. It is the synthesized influence of the separation and interaction around the flow of the train. The drag of train is decided by the flow structure around the train. As far as the flow discipline of train concerned, different shapes of the train have different flow structures, while the similar train shape has the same flow structure. Therefore, it is important to study the flow structure discipline deeply to find the best streamline shape of the train and the measures of reduction of train drag [13, 14]. Train-induced flows include the flow around fore-body and after-body of the train, the flow underneath the train, and the flow around bottom and side of train and the connecting parts.

1.5. Statement of the Problem

Train drag is divided into the aerodynamic drag, the sliding force between the wheel and rails, and the friction force caused by the pantograph system. According to the results of several full scale tests, for the bluff shape train running at a speed of 120 km/h, the aerodynamic drag is about 40% of the total drag, which climbs up to 75% when the speed reaches 160 km/h. For the train with the length of streamline shape more than 5 m (train body mount system and a skirt system to smooth the structures underneath the train), the aerodynamic drag is about 75% of the total drag when the speed of train is 200 km/h. For the train with the length of streamline shape up to 10 m, the aerodynamic drag is about 75% of the total drag when the speed is 300 km/h [13]. Therefore, aerodynamic drag plays an important role for the high-speed train. In order to reduce the train drag and the energy consumption, detailed understanding on the aerodynamic drag and its precise evaluation are of great importance. However few researches are done on regional or low speed train, even though the drag effect on the energy efficiency plays great role.

This paper tries to investigate the aerodynamic performance of Ethiopian National Train specifically Addis Ababa Dire-Dawa passenger train by ANSYSFLUENT 12.0. For the

analysis two HDX1C locomotive and one passenger car which has operating speed of 120 km/hr.'s are used. Numerical simulation and theory analysis are adopted to study the aerodynamic drag of Addis Ababa-Dire Dawa passenger train, performance against cross wind and its shape optimization are done in this work. The energy consumption aspect of drag is also presented.

1.6. Objective of the Study

1.6.1. General Objective

The objective of this paper is to examine the aerodynamic performance of Addis Ababa Dire-Dawa passenger train using commercial CFD-software (ANSYS-fluent 12.0). The stability against cross wind from -30 to 60 degree will be checked. The result will be analyzed and an optimum profile will be developed, a brief comparison of the aerodynamic performance of the two will be conducted. Energy aspect of drag reduction also explained.

1.6.2. Specific Objective

With the data and analysis of the simulations complete, the following questions will be resolved:

- How good is the aerodynamic performance of the train regarding lift and drag, and stability against cross wind?
- What are the differences in aerodynamic performance between the two?
- Are there any weak aerodynamic areas on the trains?

Since there exists previous CAD-data, modeling of CAD-models needed for the CFD-simulations will be made from the data from ERC (Ethiopian Railway Corporation).Optimizing the head shape of the Addis Ababa Dire Dawa passenger train, an efficient optimization approach is proposed. The CFD analysis by solving Navier-Stokes equations is coupled with optimization calculation based on the multi-objective optimization design method, meanwhile the computational fluid dynamics and response surface methodology is also introduced into the design flow, which greatly shortens the time consumption for geometry regeneration and flow field re-meshing. As a result, the efficiency of the optimization calculation is highly improved. Statistical analysis is done to the designs in the design space, and the correlation between the design variables and the objective is

studied to find out the key variables that most affect the objective. Response surface analysis is also performed to get the nonlinear relationship between the key design variables and the objective with the multi-objective algorithm. Finally, after the optimization, an aerodynamic performance comparison between the optimal shape and the original shape compared. Better shape will be developed to use the former at the higher speed. Lastly the drag of the two will be compared to check the stability of the train. Finally aerodynamic shape optimization advantages on efficiency of energy utilization will be analyzed.

1.7. Scope and limitations of the study

The scope of this study is mainly concentrated on aerodynamic perspective of the resistance mainly on drag and lift. As the main part of the total aerodynamic resistance lies on the frontal part of the train surface the main focus of the study is around the train nose.

The limitations of the studies are mainly because of unavailability of detailed drawing of the train body. In which the result may be slightly different from exact solution. However as our main focus is on the shape optimization this does not have much problem. The amount of aerodynamic resistance in percent over total resistance is not included because it's difficult to calculate total resistance of the train without having resistance such as mechanical resistance, rolling resistance and so on which require detailed information of the train including dimensions and material properties.

1.8. Organization of the Study

This paper has a total of five chapters which contain introduction in the previous chapter and the following four chapters. In the introduction background of vehicle aerodynamics, train energy efficiency, advantages of drag reduction is presented. Motivation and some of the previous works on external aerodynamics by computational fluid dynamics (CFD) is included. The definition of CFD, theories and some governing equation used in fluent also highlighted in this chapter. The formation, type and reduction measures of aerodynamic drag are also introduced in this first chapter. Statement and objective of the study finishes the first chapter.

The second chapter contains literature review parts. There are few works done on this area, low speed train aerodynamics, we used the paper on medium-low in some case high speed train.

The third chapter is the main body of the study, which contains aerodynamic streamlining of the train both with and without the cross wind effect, the aerodynamic shape optimization which mainly concentrated on the reduction of drag coefficient, at the end of this chapter aspect of energy efficiency of the train is discussed.

The fourth chapter contains the results of the analysis and discusses the implications of the results.

The last chapter ends the main works of the study, which contains the conclusion of the paper and suggested future works. At the end of the paper there are references and appendices used in the study.

CHAPTER TWO: LITERATURE REVIEW

Aerodynamic issues concerning railway systems are numerous [15]. Aerodynamic noise generated by the train has a negative influence on the environment around the railway system and on the passengers inside the train. Pressure variations in tunnels increase the drag of the train significantly in comparison to open air and can cause considerable ear discomfort for passengers in the train and riding discomfort due to large dynamic oscillation of the train. Pressure waves radiate to the environment from the tunnel exit. The increased driving resistance inside tunnels increases the mechanical stress on the train. The slip stream (a very strong shear layer) formed around the moving train can cause serious accidents to persons or material located on platforms when trains pass by. Cross-winds can cause very serious accidents such as derailment. The aerodynamic drag induced on the train affects the economics of the railway system considerably and limits the maximum speed. High speed trains (HST) are in general shaped in a very good way in regard to minimizing the aerodynamic drag. However, still it is responsible for the consumption of some 40-50% of the total energy put into the railway system during traction for a typical HST. For regional type (RT) of trains, the aerodynamic drag contributes less to the total energy consumption due to the typical lower operational speeds. In general regional trains have a worse shape from an aerodynamic drag minimizing point of view compared to high speed trains. The contribution to the total aerodynamic drag on a train comes from different areas of the train: skin friction drag along the train body, pantographs and other protruding objects, inter-carriage gaps, brakes, boogies and the pressure difference between the head and the tail of the train, the last one being dominating for RT trains.

To reduce the problems discussed above many researchers have done lots of work. As illustrated in our first chapter this paper only concentrated drag and drag reduction method particularly by better shape design. Taking this into consideration the following works done by some of the researchers are presented, specifically on cross-wind and shape optimization.

Chris Baker [16], considered aspects of the aerodynamic behavior of high speed trains. It does not specifically address the many aerodynamic problems associated with such vehicles, but rather attempts to describe, in fundamental terms, the nature of the flow field. The rationale for such an approach is that the flow fields that exist are the primary cause of the aerodynamic forces on the train and its components which result in a whole range of aerodynamic issues. This paper thus draws on a wide range of model scale and full scale

experimental and computational work and attempts to build up a comprehensive picture of the flow field. Attention is restricted to trains in the open air (i.e. tunnel flows will not be considered) for both still air conditions and crosswind conditions. For still air conditions the flow field will be described for a number of flow regions i.e. around the nose of the train, along the side, roof and underbody of the train and the wake of the train. Calculations of the nature of the wind relative to the train are presented for a variety of train speeds and wind speeds. For crosswind conditions, the nature of the flow field around typical trains, including surface pressure distributions, are presented. In addition the aerodynamic admittances / weighting functions for different types of train are discussed. Finally some remarks are made as to the relevance of the data that has been presented to current issues in train aerodynamics.

Asress Mulugeta Biadgo [17] studied Aerodynamic Characteristics of High Speed Train under Turbulent Cross Winds, a Numerical Investigation using Unsteady-RANS Method.. Hence, increasing velocity combined with reduced mass of modern high speed trains poses the question of influence of strong cross winds on its aerodynamics. Strong cross winds may affect the running stability of high speed trains via the amplified aerodynamic forces and moments. In this study, simulations of turbulent cross wind flows over the leading and end car of ICE-2 high speed train have been performed at different yaw angles it shows the train aerodynamic problems are closely associated with the flows occurring around train. The flow around the train has been considered as incompressible and was obtained by solving the incompressible form of the unsteady Reynolds-Averaged Navier-Stokes (RANS) equations combined with the realizable k-epsilon turbulence model. Important aerodynamic coefficients such as the side force and rolling moment coefficients have been calculated for yaw angles ranging from -30° to 60° and compared to results obtained from wind tunnel tests. The dependence of the flow structure on yaw angle has also been presented.

The computed aerodynamic coefficient outcomes using the realizable k-epsilon turbulence model were in good agreement with the experimental data for almost all yaw angles. This study shows that unsteady CFD-RANS methods combined with an appropriate turbulence model can present an important means of assessing the crucial aerodynamic forces and moments of a high speed train under cross wind conditions. The aerodynamic data obtained in this study can be used as a starting point for more advanced studies that investigate influence of strong cross wind on the aerodynamic coefficients of high speed trains while moving either on flat ground or in other dangerous scenarios such as sites with tall viaducts and high embankments.

Veera Venkata Sunil Kumar Vytla [18] under the title Multidisciplinary Optimization Framework for High Speed Train using Robust Hybrid GA-PSO Algorithm he studied that, High speed trains are the most efficient means of public transportation. However the speed of the train needs to be increased (> 350 km/hr.) to cover large distances in a short time to make it accessible to large population. With the increase in speed, number of issues related to efficiency, safety and comfort like the aerodynamic drag, structural strength, as well as the noise levels inside and outside of the train etc. need to be considered in the design of the high speed trains, hence making it a multi-disciplinary design problem. There are a large number of parameters from different disciplines that need to be tuned to identify the best design. The parameters need to be optimized to identify the best design configuration that meets the design requirements. This requires the use of robust and efficient optimization algorithms. Evolutionary algorithms have been used extensively in the engineering design optimization problems, but they suffer from a drawback of lack of robustness. One of the objectives of this research is to address the robustness issue of currently available optimization algorithms. A hybrid GA-PSO algorithm combining the benefits of both the original algorithms GA and PSO is proposed in this research. The hybrid GA-PSO algorithm was observed to be robust and accurate based upon the tests. The computer simulations required to complete the optimization of this problem are expensive both in terms of computational resources as well as time.

To minimize the computational effort an adaptive surrogate model based on kriging was used during optimization. The accuracy of the surrogate model was checked during the optimization process using the parameter called expected improvement value (EIV) and is updated whenever found to be inadequate. The optimization algorithm combined with the adaptive surrogate modeling technique is tested on Branin function and is found to be robust and efficient. The optimization of a high speed train is an MDO problem. The MDO problem can be simplified significantly if the problem can be decoupled thereby reducing the complexity of the problem. The objectives considered while finding the optimum design of the high speed train are aerodynamic drag for efficiency, structural strength for safety, and generated noise for human comfort. The objective for comfort, noise levels both inside and outside the train can be used as a decoupling objective between the aerodynamic and structural optimization. The optimization is performed sequentially. First step involves performing the shape optimization which identifies the optimum aerodynamic shape and

structural optimization is performed on the optimum shape to identify the structure strong enough to withstand the aerodynamic loads with the least mass.

A multi objective shape optimization is performed to identify the aerodynamic shape which induces least drag and generates least aerodynamic noise. Aerodynamic shape optimization requires the construction of new CAD models and some preprocessing to generate the computational mesh before the shape is analyzed. This step becomes complicated and is a hurdle when trying to automate the optimization process. Shape optimization is performed by using the shape control parameter son computational mesh and deforming the mesh along with the surface to obtain the optimum shape using commercial mesh deformation software, Sculptor. This approach was tested on a 2-D model before using it on a 3-D train model. Shape optimization is performed using a commercial CFD solver SC/Tetra. Since shape optimization is performed using mesh deformation software, there is an additional step of preparing the structure after the shape optimization is completed. Time averaged pressure loads acting on the structure are simulated using the optimum shape of the train and are mapped onto the structure. Structural optimization is performed to identify the structure that supports the optimum shape, with least mass and least noise levels inside the train. This optimization is performed using structural solver Abacus. The suggested sequential MDO approach for high speed train reduces the optimization time required to find the optimum shape and structure of the train.

Sinisa Krajnovic [19] studied Aerodynamic optimization of vehicles using computational fluid dynamics and response surface methodology. The optimization of the aerodynamics of road and rail vehicles has traditionally been handled through trial and-error design procedures, which count on the skills and experience of the designer to suggest changes in the design that are likely to yield improvements. Although such a procedure usually yield an acceptable design and use of more rigorous optimization methodology would allow the best design to be identified. The majority of numerical design optimization in fluid machinery uses gradient-based search algorithms. These methods work iteratively through the design space until the optimal design is reached. Such an approach is impractical in optimization of vehicle aerodynamics due to computational effort required for such a large number of CFD simulations.

One way of making the shape optimization of the vehicle feasible is to use the surrogate model based optimization to estimate the response of CFD simulation. These models have

been used successfully in various fields such as design of airfoils, propulsion and turbo machinery. The surrogate models give a global approximation of the response and therefore can be used in providing better understanding of the relationship between the design variables and the response. There are several different surrogate models such as response surfaces (polynomial regressions), neural network, Kriging and Radial Basis Functions. Here it only discussed the response surface model that was used in the present study. The design problem of vehicle aerodynamics has multiple objectives, i.e. drag, lift force, cross-wind stability, aero acoustics etc. Such a multi-objective optimization problem has several optimal solutions called the Pareto optimal front which can help the designers to visualize the trade-offs between different objectives and select a compromise design.

The present work presents the use of response surface approximation (RSA) for multi-objective optimization of vehicle aerodynamics. We use an example of optimization of aerodynamic properties of a two-dimensional vehicle to demonstrate an efficient multi-objective optimization procedure. The chosen object functions are drag and lift and the response surfaces are produced as a result of Reynolds-Averaged Navier-Stokes simulations (RANS) using simple two equation turbulence model.

Meng-ge Yu, Ji-ye Zhang, Wei-hua Zhang [20] studied Multi-objective optimization design method of the high-speed train head. The multi-objective optimization design method of the high-speed train head was proposed in this paper, and the aerodynamic drag and load reduction factor were set to be optimization objectives. The automatic multi-objective optimization design of the high-speed train head can be achieved by integrating a series of procedures into the multi-objective optimization algorithm, such as the establishment of 3D parametric model, the aerodynamic mesh generation, the calculation of the flow field around the train, and the vehicle system dynamics. The correlation between the optimization objectives and optimization variables was analyzed to obtain the most important optimization variables, and a further analysis of the nonlinear relationship between the key optimization variables and the optimization objectives was obtained. A parametric model of the high-speed train head is established in the present paper. The aerodynamic performance and vehicle dynamic performance of the high-speed train are calculated through the batch commands and script files. The multi-objective optimization algorithm NSGA-II is used for the automatic multi-objective optimization of the head shape, with the optimization objectives of the aerodynamic drag and load reduction factor. The proposed method can greatly reduce the design cycle of the head shape, and obtain a better head shape with good aerodynamic

performance and vehicle dynamic performance. After optimization, the aerodynamic drag of optimized train was reduced by up to 4.15%, and the load reduction factor was reduced by up to 1.72%.

Almost all of the above researches are done on the high speed train; however they also pointed out that in low speed train the problem is not easy. As it is discussed in the above section, this paper analyzes this problem on Ethiopian National Railway perspective. To do this we use all above papers to some extent. For example, from the first paper (16) we take the general overview of the aerodynamic drag over a train. As it covers money ideas, based on high speed train and it's not specific we didn't rely only on this paper. From the second paper by Asress Mulugeta Biadgo, we took the aerodynamics against cross wind, as it clearly analyze this characteristics so our discussion/analysis based on cross wind analysis take this paper as a base. The difference between our paper and this are this paper didn't consider the full scale and it uses transient or unsteady RANS method analysis for small model. In our case we use full scale and used steady state RANS because of large time it takes for convergence and large computer capacity required. This assumption is recommended if we compensate by increasing the tunnel box size for analysis. This also makes sense because the difference in accuracies of the solution is not much and our main focus is to reduce the drag by better shape optimization.

The next paper discussed is the paper by Veera Venkata Sunil Kumar Vytla; from this paper we took the general guidelines in optimizing the shape of a train to reduce aerodynamic drag. This paper uses surrogate method algorithm which requires high knowledge of mat lab and for this paper we didn't thought it's that much evident. From this paper we took the concept such as, how to decide the variation of the changing width of critical variables, nose height, width and height and maximum recommended size of the train nose dimensions taking the speed of the train into account. The paper we used for shape optimization was the paper by Sinisa Krajnovic, this paper clearly explain the steps followed in using surface response method. We took this idea from this paper mixing with multi-objective optimization method which uses approximation method and refine the concavity and convexity of the surface model by clearly defined equation (Meng-ge Yu, Ji-ye Zhang, Wei-hua Zhang).

In addition to the paper discussed above we use the paper listed in the reference section. The work done on railway engineering are not much published as other areas, hence in some cases we use the work done on aerospace engineering like aero foil, and automotive engineering

like car. Even also in such areas they are not clearly and fully published journal but there are many research going on and standardization also getting started which makes the railway engineering future bright. The literature used on the energy efficiency is listed in the reference section [21].

CHAPTER THREE: SIMULATION AND METHODS OF THE STUDY

3.1. Vehicle Aerodynamics: Numerical and Computational Evaluation Methods

Numerical evaluation methods involving vehicle aerodynamics and aero-acoustics can be done either analytically or by using Computational Fluid Dynamics (CFD). Analytical methods in solving airflow behavior realistically can be done on simple generic type flow problems in either two-dimensional or three-dimensional form. As airflow behavior gets more complex when subjected to flow around complex geometrical domain or bluff bodies, (with the presence of turbulence and compressibility effect), solving airflow properties cannot be done analytically. This is because in order to obtain its complete turbulent and aerodynamic noise source properties, full unsteady Navier-Stokes (taking into account inertia, viscous and pressure forces) together with the continuity equation (mass conservation) need to be solved.

However obtaining a direct numerical solutions of Navier-Stokes equations are still not yet possible even for modern day computers. The main reason being that gird points needed for a typical CFD model to be solved are $Re^{9/4}$. For a typical flow with Reynolds number of 10^6, it will take the computer to generate and solve equations for $3.16x10^{13}$ gird points. This is far beyond the reach of even the most state of the art supercomputers available in the world today. In order to come up with a comparable solution, steady or time averaged Navier-Stokes equation is used (called Reynolds Average Navier-Stokes equation – RANS) together with turbulence model, developed to take into closure problems involving Reynolds stresses resulting from the time averaging process. Solving for RANS, continuity and turbulence model equations can be done via Computational Fluid Dynamics (CFD) simulations.

CFD approach for turbulence modeling was first intended for the aerospace community in the 1960s and 1970s. In the early development stage of CFD for automotive applications, codes were expected to provide actual quantitative data that is similar to measured wind tunnel data. Knowing that this is not yet possible, present use of CFD in automotive are used to provide information about flow characteristics and phenomena, which dictates aerodynamic performance. However, the ultimate goal in CFD is to obtain model as flow as actual as

possible and current and future research on CFD is ongoing in order to achieve that goal. Furthermore, current applications of CFD in the automotive industry are determined by economic viability. To be economically viable, the codes should be able to simulate the correct physics of the flow and at the same time achieve computational turnaround time that is the same or less than that of a wind tunnel test cycle time. Ahmed [22] has showed that for a typical vehicle, current testing time taken in a wind tunnel in order to achieve desired level of c_d reduction has increased. This will be an expensive exercise for automobile manufacturers. With the reduction on computational cost, aerodynamic simulation by using CFD, being run at a faster turnaround time will only be at a fraction of the cost. In this study aerodynamic simulation using RANS method is used.

3.2. Aerodynamic Simulation Method

External aerodynamic simulations using computational fluid dynamics (CFD) are well established tools in the product development process for the automotive and aerospace industries [22]. CFD simulation technology helps engineers to understand the physical phenomena taking place in their design and provides an environment to optimize the performance with respect to certain design criteria. In the automotive domain for example, the aerodynamic forces, e.g. lift, drag and cross force, have a strong impact on the vehicle's fuel efficiency and handling behavior. CFD can be leveraged to analyze these forces and to determine an optimal design.

In general, external aerodynamic flows exhibit a transient behavior, especially for road vehicles. However, the simulations are often performed in steady state mode to reduce the computer run time and to increase the turnaround time for different designs.

The external aerodynamics plays an important role in the development process of modern automotive. The vehicle's performance (e.g. fuel consumption), its stability (e.g. cross wind sensitivity) and the vehicle's cooling system (e.g. engine cooling) are all influenced by aerodynamic loads. Furthermore, the driver's comfort (e.g. interior cabin noise due to vortices) and the driver's visibility (e.g. performance of wipers) depend on the external flow field.

The automotive industries apply wind tunnel experiments and computational fluid dynamic (CFD) simulations to study the aerodynamic loads on their vehicles. Fast computer systems and sophisticated numerical methods allow the investigation of complex flow structures in an

acceptable turnaround time. As a result, CFD simulations became more and more popular and the number of wind tunnel experiments during a vehicle's development process got reduced. Wind tunnel testing is still an essential step in the automotive industry and a combination of virtual and experimental testing will always go hand in hand.

The general workflow to perform an aerodynamic CFD analysis of a vehicle can be described in four steps

1. Model preparation (e.g. geometry cleanup or surface meshing)
2. Volume meshing
3. CFD case setup and solver run
4. Post-processing

The geometry used for the analysis is shown in figure 3.1; it was taken from ERC technical department [appendices]. Some of the detailed dimensions are taken by assumption because of the unavailability.

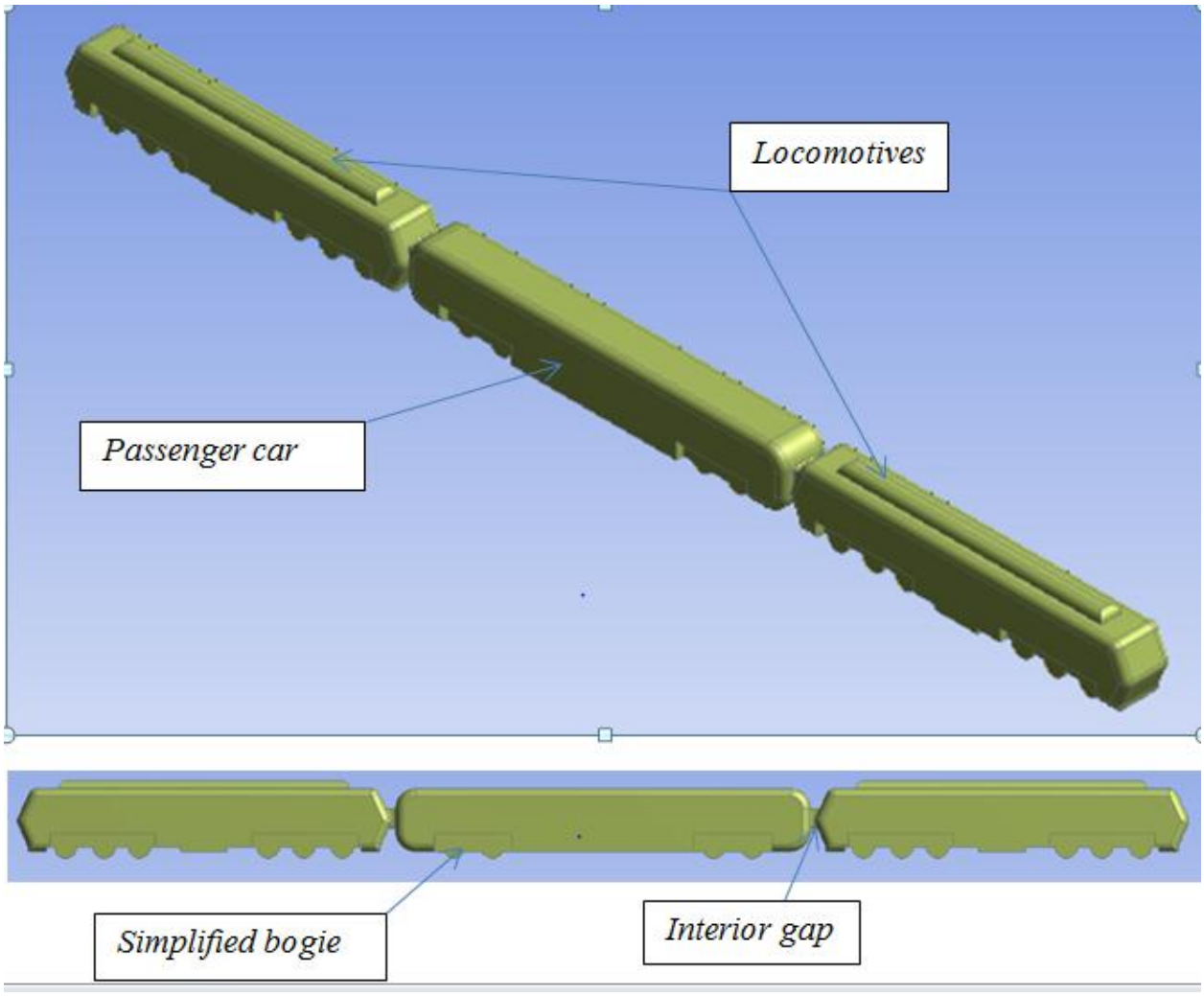

Figure3.1: Ethiopian National Train (HDX1C locomotive and hard seat passenger car)

3.2.1. Aerodynamic Simulation of the Train with-out the effect of Cross-wind ($\alpha = 0$)

3.2.1.1. CFD Setup

CFD analysis is performed using a commercial CFD solver, ANSYS FLUENT12.0 flow solver based upon finite volume approach. The software has a number of turbulence models available which are validated thoroughly. A 3-D flow problem using the LES model for a model as big as a train is not practical because the computational requirements will be enormous and simulations will take a very long time to complete making the flow problem virtually unsolvable.

Instead the flow is predicted using steady Reynolds Averages Navier Stokes (RANS) model using the standard k-epsilon turbulence model. The speed of train considered in this study is

120Km/hr. which is equivalent to 34 m/s. This is equivalent to a Mach number of less than 0.3 [23] and hence the flow can be assumed incompressible. The Reynolds number of the flow based upon the train length is around$7.2*10^6$[24, 18].

3.2.1.2. Numerical Simulation Method

The simulation/analysis was done based on the double precision option. Since double precision has 8 decimal places the double precision and serial processing methods are good enough for this project [25].The calculation is pressure based since for low speed we can assume incompressible flow pressure based is better than density based. The time used was steady as transient is very difficult for such large geometry and it takes lots of time to converge. The velocity formulation is absolute type rather than relative. Model type used in this paper was k-epsilon (2eqn.), realizable, non-equilibrium wall functions and the material used was air at operating condition of 76kpa and 298.5k. The solution method used in this paper is simple method type as our main focus is on the overall characteristics of the flow not the accuracy.

3.2.1.3. Description of the model Geometry, Computational domain and mesh

The computational domain and the boundary conditions used in the analysis are shown in figures 3.2 and 3.3. The length of the train model considered in this study is 25m wagon and two 22.5m locomotive with 0.3m gap for coupling space. The total length of the model considered is 70.6m. Though there is little aerodynamic effect in between rear and front the train it's logical to consider one of the wagon attached. The computational domain is extended by two lengths of train both upstream and downstream of the train. The total length of the computational domain is around 3 times the length of the train. The computational domain is also extended in the transverse directions by 0.5 times the length of the model each on either side of the train. The height of the computational domain is also extended by about 0.5 times the length of the model. A small gap of 0.1m is modeled between the train body and the ground to account for the wheel/rail height if not considered [26]. One of the assumptions made about the flow is that the wind flow is normal to the train ($\alpha = 0$), based upon the assumption condition that the train is traveling in a straight path. Hence the inlet is set as velocity condition and is set as uniform velocity of 34m/s for 120km/hr speed train. The outlet is modeled as static pressure boundary condition with the outlet pressure set as 0pa. The boundary surfaces on the sides and top of the train are modeled as free slip walls or

symmetry, no resistance to the flow. The ground is modeled as a stationary wall with the wall velocity equal to 0m/s in order to maintain the relative velocity between the train and ground when the train is moving. Train is modeled as a wall with shear stress wall boundary condition. For meshing we use the automatic patch conforming/sweeping method. The mesh refinement is done around train surface for better resolution of the result for CFD analysis. The computational mesh has around 1.25 million elements and is shown in figure 3.4a. A 3-D incompressible flow is solved to determine the induced drag, generated lift and to predict the aerodynamic noise. Most of the work done on shape earlier is limited to steady state prediction of lift and drag; however, in reality the forces acting on a 3-D train body are periodic in nature. The model created on the CatiaV5 and its tunnel duct is shown on figure (3.2, 3.3) below.

3.2.1.4. Boundary Condition

As roughly discussed in the previous section and shown in the following figure (3.3) fluent have some integrated boundary condition such as wall and symmetry, for external bluff body simulation, so that as we specify it at the meshing phase it will recognize it [27].In this particular project we use symmetry boundary condition for the two sides and top of the duct. For the train surface and ground no-slip boundary condition. For inlet we use inlet velocity that 34 m/s and specification of turbulent intensity and turbulent viscosity ratio 1%, 10 respectively. For outlet Neumann boundary condition that is 0pa and specification of backflow turbulent intensity and backflow turbulent viscosity ratio 5%, 10 respectively [25].

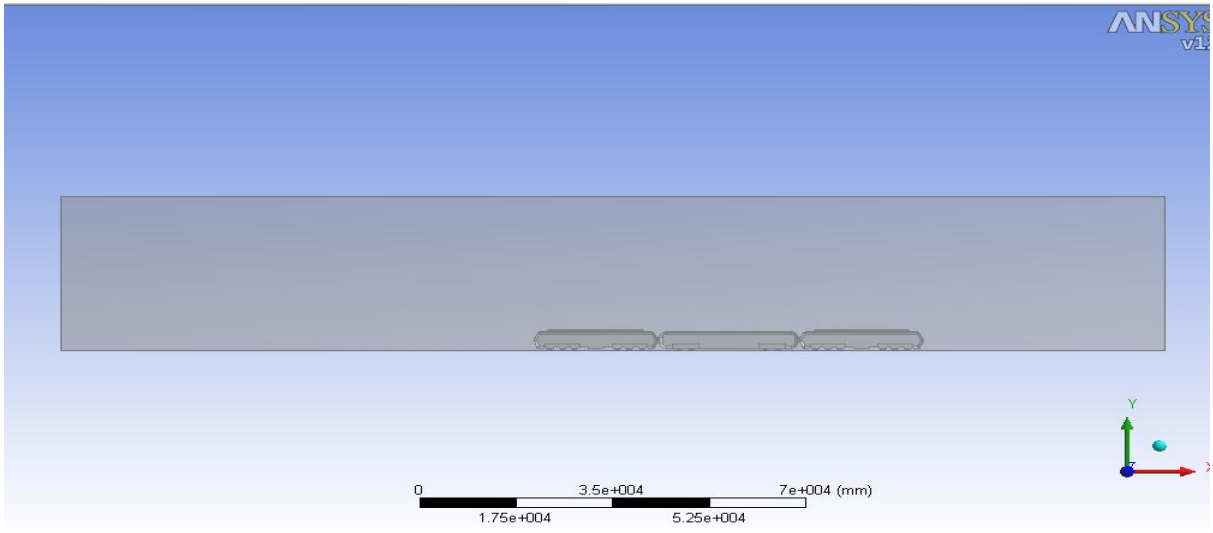

(a)Side view

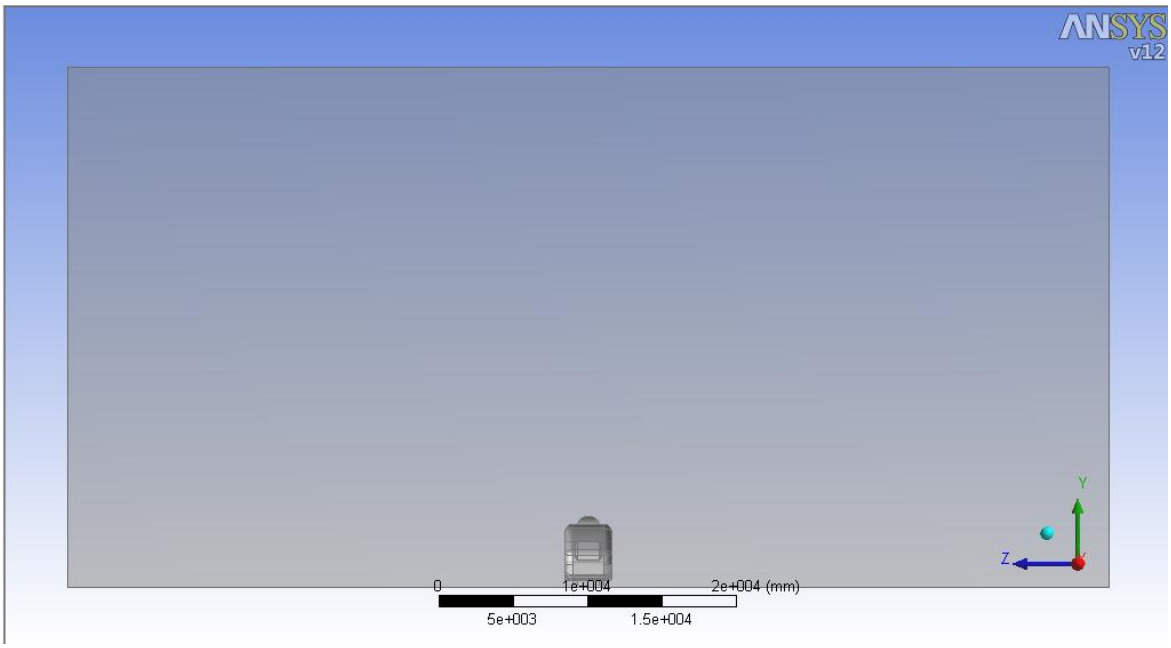

(b)Front view

Figure3.2: Computational domain of a 3-D train

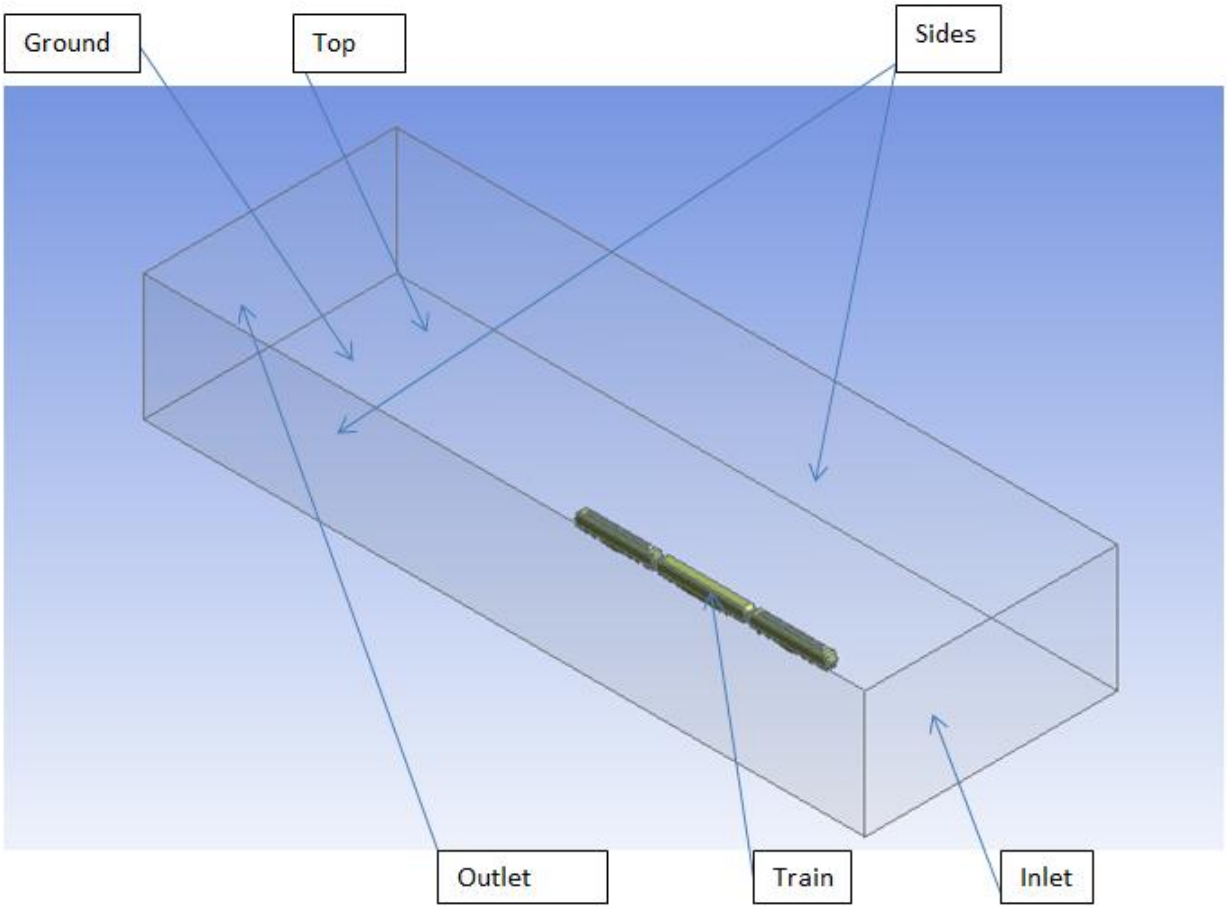

Figure3.3: Boundary conditions used in CFD analysis

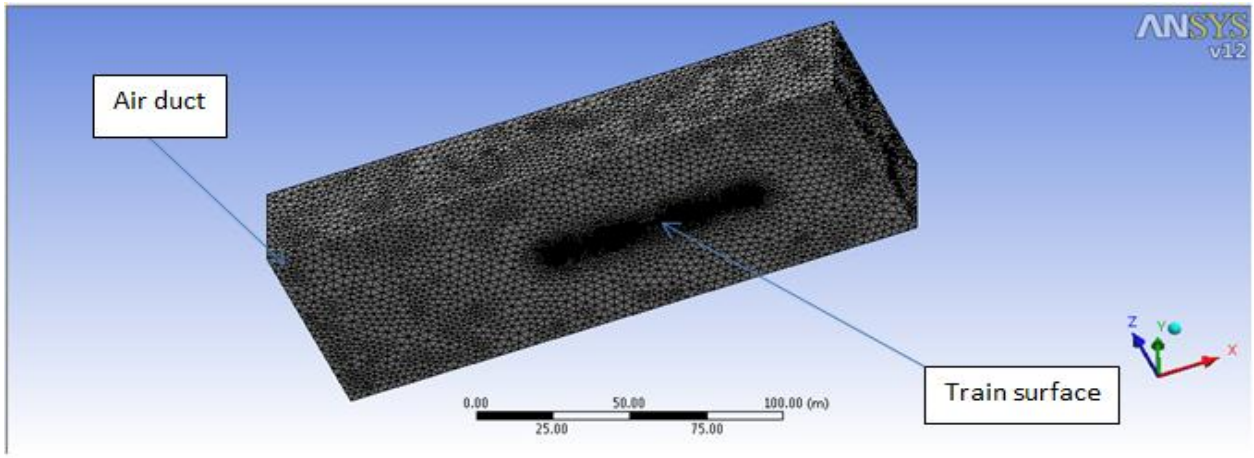

(a)

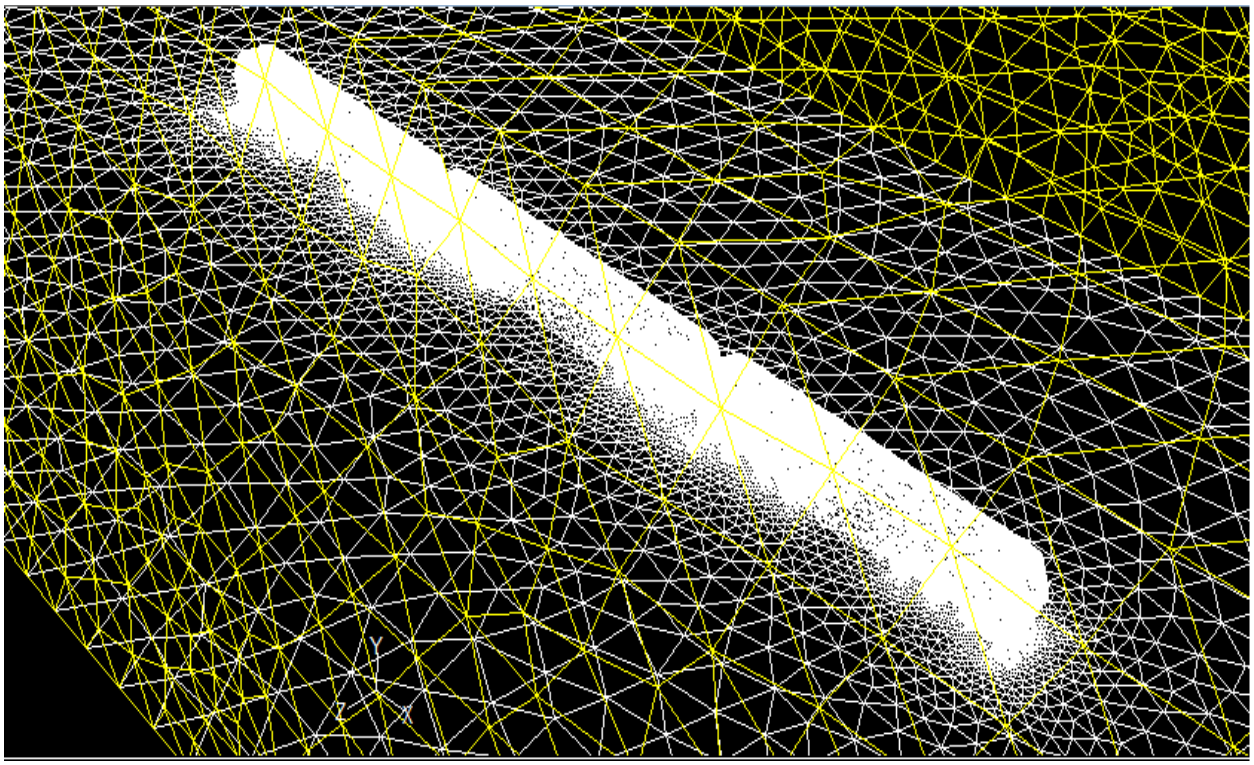

(b)

Figure3.4: Meshed train surface inside the air duct

3.2.2. Aerodynamic Simulation of the Train With the effect of Cross-wind ($\alpha \neq 0$)

Although trains may be considered the safest existing ground vehicles, there has always been the occasional derailment due to strong side winds, mostly on islands [28]. According to meteorologists, the current global warming leads to ever stronger winds meaning such accidents are more likely to happen not only in coastal areas but even in the very heart of larger continents. This is how a commuter train was blown over in Austria recently [28], only 5 years after a similar accident happened in Belgium. The present tendency of reducing the weight of trains obviously contributes to their increased side wind sensitivity. The dramatic increase of the train speeds that we have witnessed in Europe and Japan in the last decade further exacerbates the problem. Finally, the long and slender noses that are required for high speed trains are unfortunately particularly sensitive to cross winds, as has been demonstrated by many wind-tunnel tests. This is due to the large areas of negative pressures on the leeside of such long noses. This problem is not the problem of only high speed train at low and medium speed train it's always become the cause for derailment especially on curves and embankments. This study focuses on the stability characteristics of the Ethiopian National train against cross wind. Mostly this is done through tests [29, 28] but CFD is also another option. In this study we use CFD simulation method.

3.2.2.1. CFD Setup

As discussed in the above section increasing velocity combined with reduced mass of modern trains poses the question of influence of strong cross winds on its aerodynamics [17, 29, 30]. Strong cross winds may affect the running stability of the trains via the amplified aerodynamic forces and moments. In this study, simulations of turbulent cross wind flows over the leading and end locomotives and a car of hard seat passenger train of AA-DD train have been performed at different yaw angles. The train aerodynamic problems are closely associated with the flows occurring around train. The flow around the train has been considered as incompressible and was obtained by solving the incompressible form of the steady Reynolds-Averaged Navier-Stokes (RANS) equations combined with the realizable k-epsilon turbulence model [9]. Important aerodynamic coefficients such as the side force and rolling moment coefficients have been calculated for yaw angles ranging from -30° to 60° and compared to results obtained from no-cross wind result. The dependence of the flow structure on yaw angle has also been presented.

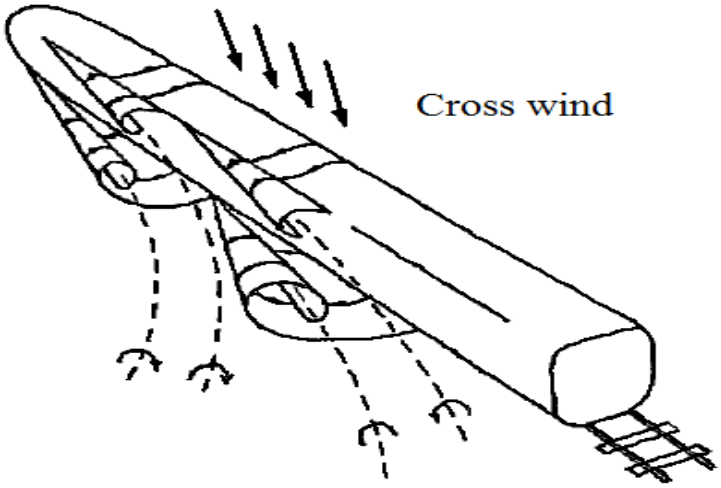

Figure 3.5: Flow behind a train in a cross wind [17]

3.2.2.2. Numerical Simulation Method

In a similar fashion to the experimental set up and also the same to no cross wind case, the numerical simulation scenario consists of a stationary train exposed to a constant cross wind of 34m/s at different yaw angles ranging from -30° to 60°.Because of the symmetric nature of the geometry of the train right and left side is equal, hence we only analyzed the effect of $\alpha = 30, 45\ and\ 60\ degree$ For the numerical simulations the commercial CFD software ANSYS FLUENT 12.0 was used (same to above). The detailed numerical simulation procedure such as the model train and computational domain creation, the mesh and boundary conditions are discussed below.

3.2.2.2. Description of the model Geometry, Computational domain and mesh

Full-size trains are not often used (same to the above) for aerodynamic studies owing to their geometrical complexities; instead, simplified, shortened models are used. Performing numerical simulation for a complete train with a length of more than 70.6m to include the entire car by turbulent method requires more advanced computational resources than those available. In addition, since the flow structure downstream of a certain distance from the nose of the train (less than one coach length) is more or less constant, a decrease in length does not alter the essential physical features of the flow [9, 17]. The model studied in this work is the same to the one used above i.e. Hard seat AA-DD passenger train which consists of the leading locomotive and end locomotive, middle car and inter-car gap. The model geometry

has total length of 70.6m, width of 3.105m and height of 3.783m including wheel. The model has been created with simplified bogies as shown in Figure 3.6on CatiaV5.

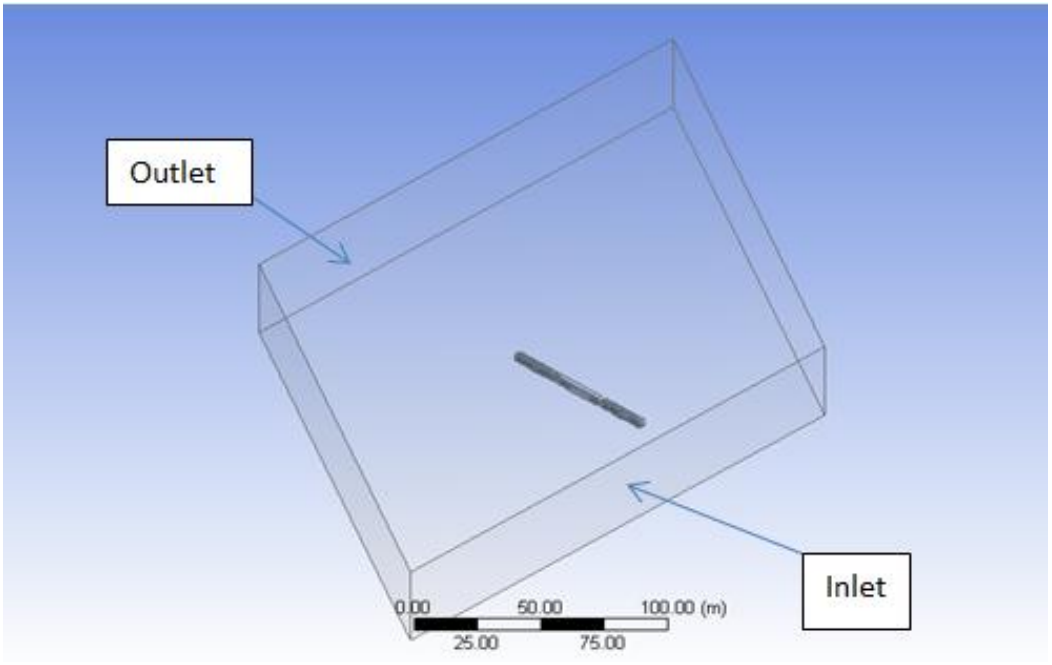

(a) Model α = 30

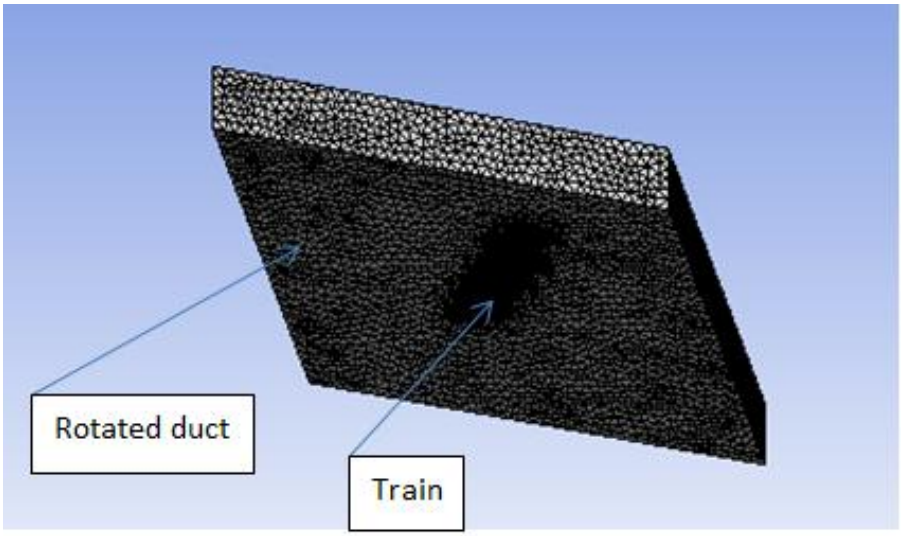

(b) Mesh

(i) When the tunnel duct rotated at 30 degree

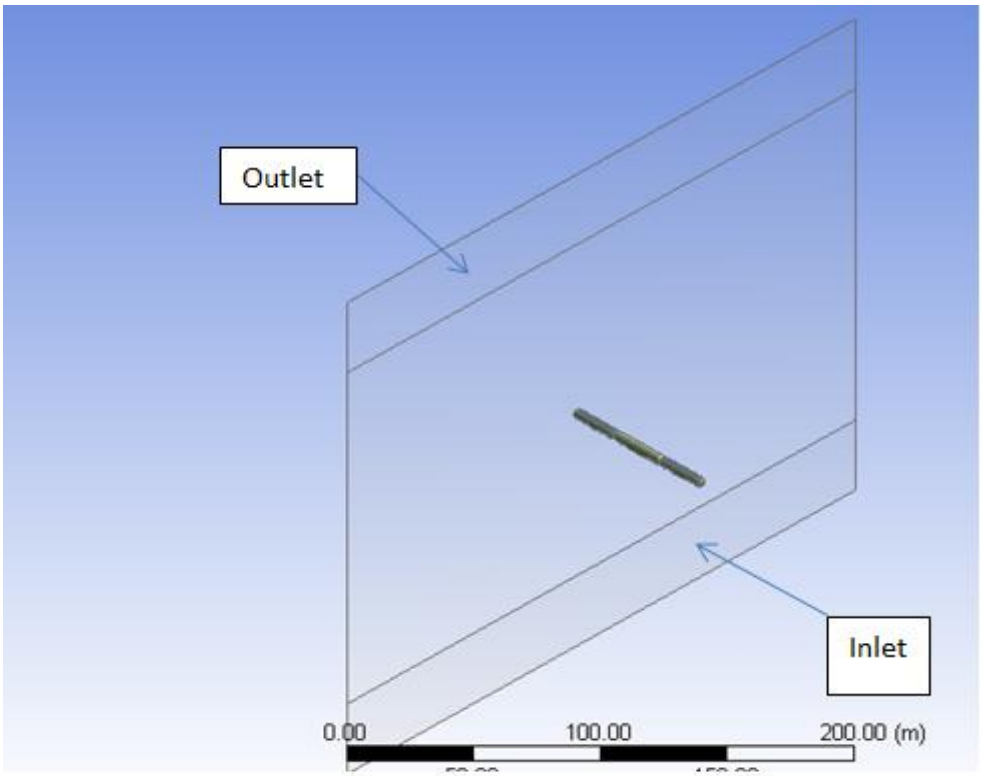

(a) Model$\alpha = 45$

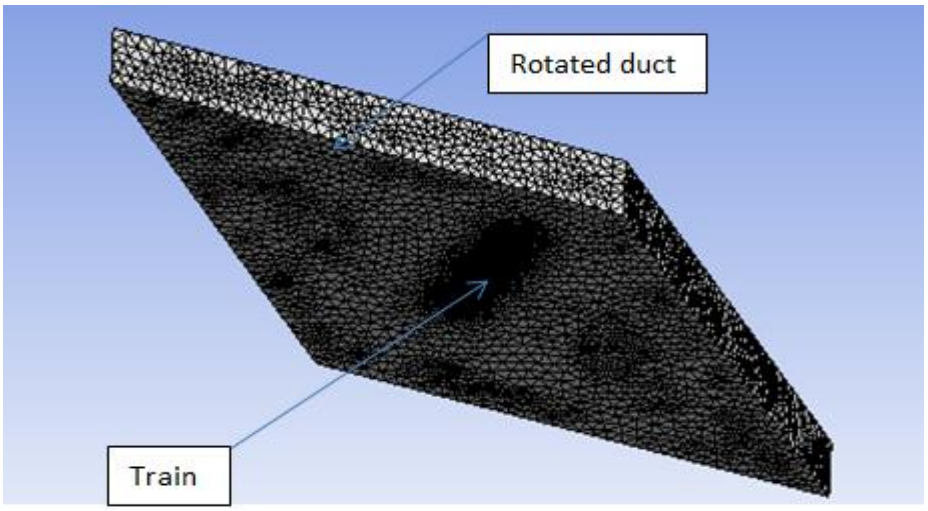

(b) Mesh

(ii) When the tunnel duct rotated at 45 degree

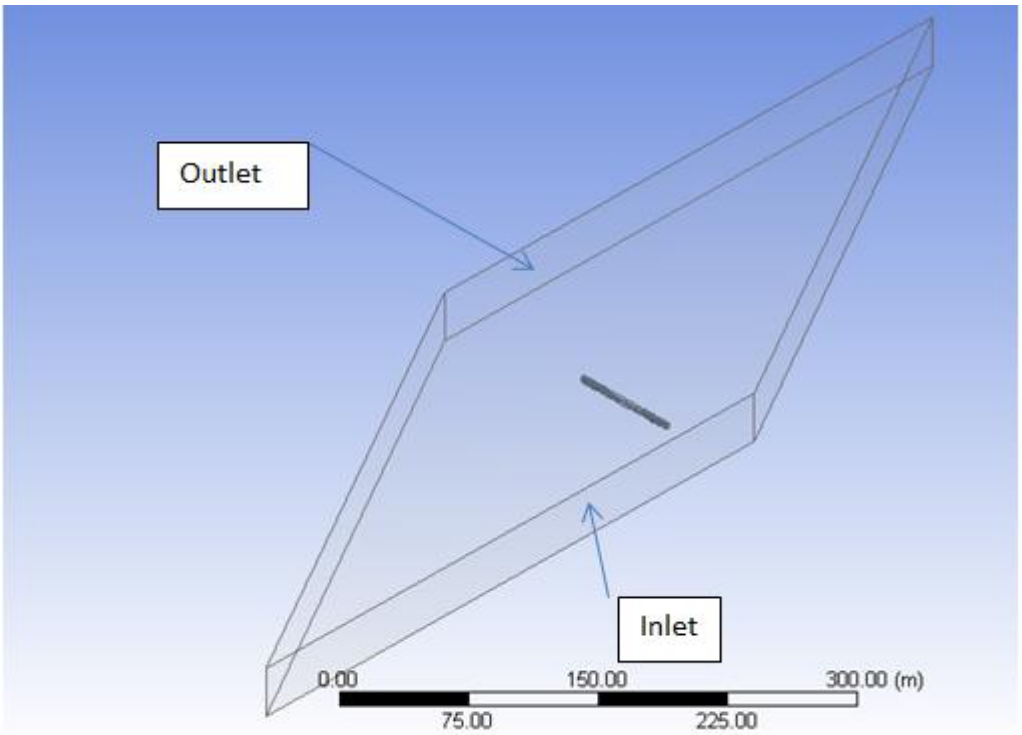

(a) Model α = 60

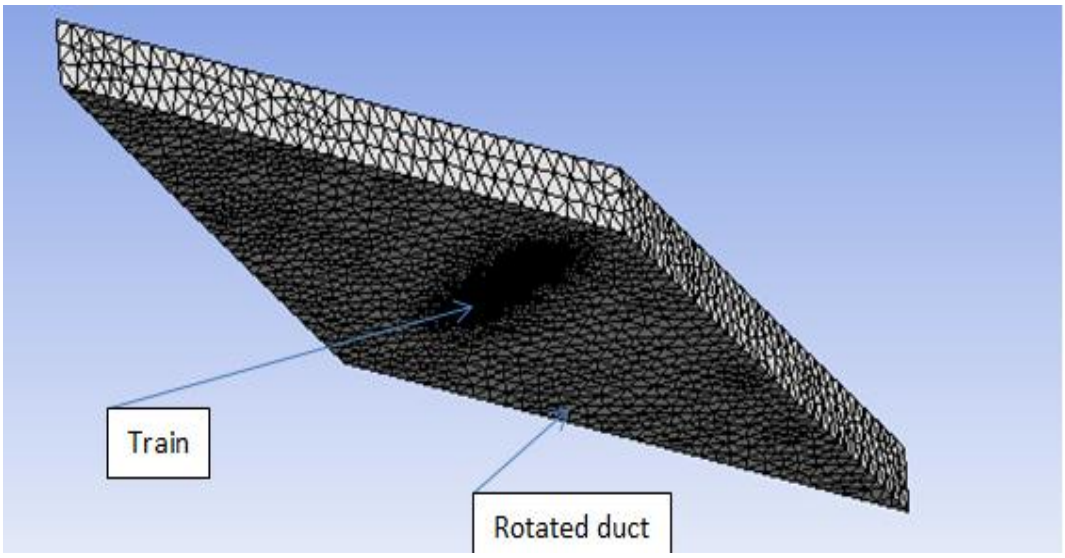

(b) Mesh

(c) (iii) When the tunnel duct rotated at 60 degree

Figure3.6: Leading and rear locomotives, interior-gap and middle car model with simplified bogie and the tunnel duct rotated at degree of α

Because of the symmetric nature of the geometry the other rotation in the negative directions are not included in the analysis. So the values at 30 and -30, 45 and -45, 60 and -60 degrees are the same.

The moment reference point is set to be located at the above ground level in the midway of the train length. The coefficients for the aerodynamic forces and moments have been obtained using a fixed reference area of 12.468m^2 which corresponds to the cross-sectional area of the train model and reference length of 3.105m which presents the width of the train model.

After the basic shape of the train has been created; a parallelepiped computational domain (Figure 3.6) of the following dimensions: height of 35m, width of300m and length of300m created simulating the wind tunnel working section. In the computational domain, the model can be rotated in the x-y plane by the required yaw angle for simulation. By increasing the size of the tunnel box the distance between nose of vehicle and the inlet boundary is sufficient to ensure that the velocity and pressure fields are uniform at the inlet and to allow the flow to develop by the time it reaches the train. The model is also sufficiently far from the top and side walls to minimize near wall effects.

3.2.2.4. Boundary Condition (same to the no cross wind case)

The flow enters the domain with a uniform velocity of 34m/s. The Reynolds number based on the inlet flow velocity and the width of train model was around $7.2*10^6$. No-slip boundary conditions were used on the train surface and the ground floor meaning that the velocity is zero. Symmetry boundary conditions were used on the top and side walls. On the outlet, a uniform Neumann boundary condition is applied, meaning that the pressure gradient equals zero. This allows the flow to pass through the outlet without affecting the upstream flow, provided that the upstream distance to the aerodynamic body is large enough. The realizable k-epsilon model was used for the turbulence closure. On the ground and solid surfaces, the non-equilibrium wall functions were used to determine the boundary turbulence quantities. The conventional SIMPLE algorithm was used to solve the coupled equations, where several iterations are performed to ensure convergence.

3.3. Shape Optimization and Preliminary Parameters optimization by ANSYS Fluent

As discussed in the above sections in both aerospace and automotive industry, aerodynamics plays a critical role in vehicle design. Shapes and designs are optimized to obtain the lowest drag possible. One way of expressing drag is by using drag coefficients. The drag coefficient is a dimensionless number used to represent the overall effects of shape, inclination, and other flow conditions. Experiment and simulation was conducted to become more familiar with the effects an object' shape has on drag. It is proven that elliptical shape has better drag performance [32].

In this study before directly went into the shape optimization using the above concept the original ENT profile was modified so as it will be expressed by three critical point spline (figure 3.7). Then by varying the three variable and refining the concavity and convexity of the curve the train nose will be optimized.

3.3.1. Aerodynamic Shape Optimization of Train Head: Method of Multi-Objective Approximation, using Computational Fluid Dynamics and Response Surface Methodology

Shape optimization is not easy task and it requires lots of resources and time as indicated on the literature part. But even though it is difficult to get the best optimized dimension we can still get the better aerodynamic performance by approximation method. Many researches have been done on shape optimization in different method [18, 26, 34, 35, 36]. In this paper we used surface response methodology to approximate the result from multi objective variables. To reduce the computational time and leave the use of mat lab program we considered the variables which are only very sensitive to the drag. The variables considered in this analysis were the upper length of the nose, lower length of the nose and the height of the nose, which made the 2-D cross-section of the model train. Shape optimization of a 2-D train model was performed using a base shape as shown in Figure 3.7. CatiaV5 is used to provide the shape control parameters and the designs profile for CFD analysis.

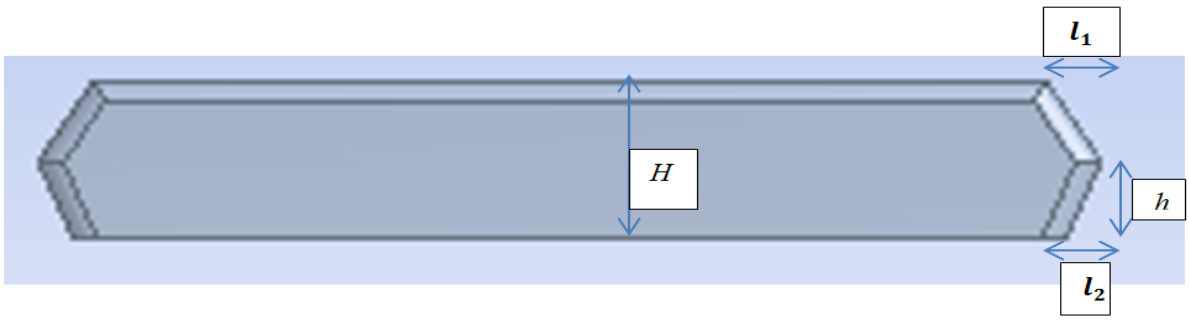

Figure3.7: The simplified initial model

The simplified initial model (equal to model number 1) shown on figure 3.7 is used as base shape for shape optimization.

The advantage of using CatiaV5 is that we don't need to remodel the new shape, We directly take the new control points from excel.

The objective is to identify the nose shape that induces the least amount of drag and limited lift; also generates the least amount of aerodynamic noise. The shape optimization of train is a multi-objective optimization problem, where the objectives are to minimize the aerodynamic drag induced and to minimize the aerodynamic noise generated because of the air flow over the body of the train. The second objective, noise, for our case is at low speed train noise is not much of concern and we concentrate on minimizing drag [18, 34, 35, 36] i.e.$min. Fdrag$ which is the same as decreasing drag coefficient.

The selections of control parameters are to control the geometry of the train by keeping the total height and length of the train and varying the nose curve length and curve intersection point [18, 35, 36].

$$0.164\text{m} \leq l_1 \leq 2.164 \text{ For} dl_1\text{=0 to 2m}$$

$$0.225 \leq l_2 \leq 1.225\text{m For} dl_2\text{=0 to1m}$$

$$1.186\text{m} \leq h \leq 2.5\text{mFor dh=0 to 0.657m}$$

Where l_1 is the horizontal length of upper curve (c_1) and l_2 is the length of the lower curve (c_2) and h is the height of the nose up to the point which connect c_1 and c_2,$dl_1$is change in length of upper curve,dl_2 is change in lower curve length and dh change in nose height.

One design requirement that separates trains from that of planes is the limitation on generated lift. For the safe operation of the train the lift generated cannot exceed a certain value, if the design generates too much lift that results in the unsafe operating conditions for the train especially when there is a strong cross wind. Similar to the design of race cars, where the design is modified to produce downward force for better traction, there is a restriction on the amount of lift generated for trains for safe operation.

Along with the constraints on the geometry there is a design constraint on the lift generated by the nose shape, the lift generated should not exceed the lift generated by the base design [18].

The constraint on the lift is expressed as:$lift \leq limit$.

3.3.2. Optimization Process

There are five steps in optimization used in this method:

Geometric parameterization

First step of every shape design process is to choose design variables. Keeping the number of design variables as low as possible is important for the computational cost of the design procedure. Vehicle shapes are today quantified using modern computer aided design (CAD) models and their description can be presented using complex mathematical description (using B-splines).It is better for an optimization purpose if the shape can be described with traditional design variables such as height, length, radius etc., which can then be translated by the computer into a CAD model. However there is today no optimal way to quantify shapes of ground vehicles today and different choices of design variables have to be compared against each other in order to find the best parameterization.

Design of experiments (DOE)

A design of experiment is a sequence of experiments (numerical experiments in our case) that will be performed. This is a critical step as the quality of the response surface approximation is dependent on the choice of the points in the design variable space from which the model will be constructed.

There are several different design strategies (for the review see e.g.[18, 34, 35, 36]) and here the Faced Centered Composite Design (FCCD) is chosen to pick the design data points.

Numerical simulation at design points

Here the CFD simulations of the designs chosen in DOE are performed. This is the most costly step (in terms of both computational resources and the men power) in the optimization process and consists of preprocessing (making computational meshes), numerical calculations and post-processing (analysis of the results). The choice of the numerical method (numerical scheme, turbulence model, steady or unsteady solver) is essential for the success of the optimization process as the computer calculated response is used for the construction of the model.

Reconstructing the selected model and checking the concavity and convexity of the selected model

The following equation is adopted for the deformation [20]:

$$y_{c,new}(i) = y_{c,old}(i) * \left(1 + \frac{dy_c(i-1)(n_c - i)}{\left((i-1)(i-1) + (n_c - i)(n_c - i)\right)}\right) \quad \ldots\ldots\ldots\ldots\ldots\ldots\ldots\ldots 3$$

Where, $y_{c,new}$, $y_{c,old}$,i, n_c is y coordinate of the curve after the deformation, before deformation, coordinate point and number of coordinate points respectively.

3.3.2..1.Geometric Parameterization of the Train

In the present paper we choose to describe the shape of the front of the train using three length variables. This is by no means the optimal description but as our train is low speed train it is sufficient for the purpose of our investigation of our models in optimization process [34, 35, 16, 18, 20].The geometry of the train is presented in Figure 3.7. The length and the height of the car are chosen as $L = 22.5\text{m}$ and $H = 3.783\text{m}$ respectively. The ground clearance is$c = 0.1\text{m}$. The objective of the present work is the aerodynamic optimization of the nose of the train shown in Figure 3.7. $l_1 = 1.164$,$l_2 = 0.725$ and h $= 1.843$

The three design variables are:

$$2.164\text{m} \geq l_1 \geq 0.164\text{m}, a_1 = 2.164\text{m},\ a_2 = 1.164\text{m}, \text{ and } a_3 = 0.164\text{m}$$

$$1.225\text{m} \geq l_2 \geq 0.225\text{m},\ b_1 = 1.225\text{m},\ b_2 = 0.725\text{m} \text{ , and } b_3 = 0.225\text{m}$$

$$2.5\text{m} \geq \geq \text{h} \geq 1.186\text{m},\ h_1 = 2.5\text{m},\ h_2 = 1.843\text{m}, \text{ and } h_3 = 1.186\text{m}$$

3.3.2.2. Design of Experiments (Numerical Experiment)

In the present study we are using center composite design (CCD). This DOE was originally constructed for physical experiments but is often used for the design of computer experiments. CCD is a two level factorial design containing two 'star' points at ±D for each factor and n center points. In the case of three design variables we have that the 'star' points are located in the center of the faces of the cube resulting in a so called Faced Centered Composite Design (FCCD). This technique generates $2^{\mathbf{N}} + 2\mathbf{N} + 1$ design points, where **N** is the number of design variables [18]. This is the main drawback of this DOE as the number of design points increases fast with the number of the design variables. In our case of three design variables a total of 15 design points were obtained which is a manageable number of designs. These designs are presented in Table below.

Table3.1: Design experiment (numerical experiment)

case	l_1	l_2	**h**	**combination**
1	0.164	0.725	1.843	a2,b2,c2
2	1.164	1.225	2.5	a2,b1,c1
3	1.164	0.725	2.5	a2,b2,c1
4	1.164	1.225	1.843	a2,b3,c3
5	1.164	0.225	1.843	a2,b3,c3
6	1.164	0.225	1.843	a2,b3,c2
7	1.164	0.725	1.843	a2,b2,c3
8	2.164	1.225	2.5	a1,b1,c1
9	2.164	1.225	1.184	a1,b1,c3
10	2.164	0.225	2.5	a1,b3,c1
11	2.164	0.225	1.184	a1,b3,c3
12	0.164	0.225	1.184	a3,b3,c3

13	2.164	1.225	1.843	a1,b1,c2
14	2.164	0.725	2.5	a1,b2,c1
15	2.164	0.725	1.843	a1,b2,c2

The 15 model generated are shown in the figure below with their sequence of model number.

no.	Model	no.	Model
1		9	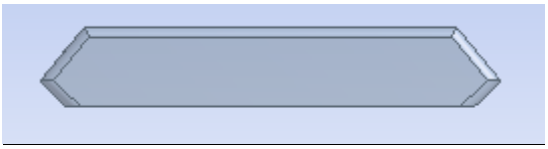
2		10	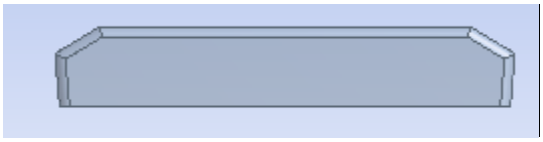
3		11	
4	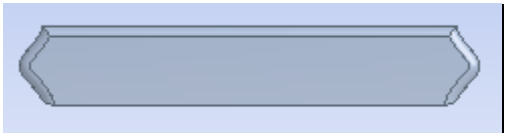	12	
5		13	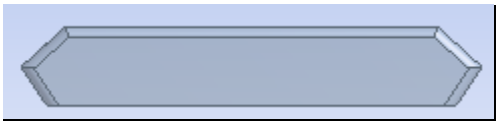
6		14	
7	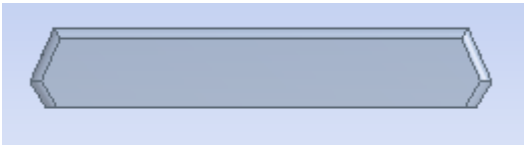	15	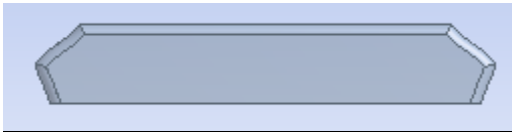

8		Plane	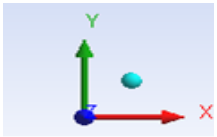

Figure3.8: Geometric models

3.3.2.3. Numerical Computations at the Design Points

Although the RANS technique can use large number of turbulent models developed during last four decades which often produce large differences in the quality of predictions, we shall here use simple κ_ε model with non-equilibrium wall functions. It is possible that use of some other turbulence model would result in different optimal solution but the topic of the present work is the optimization by approximation method we do that at the final optimized solution model.

As the result in table below shows model number 8 has better drag performance which has lower drag value.

Table 3.2*:* Numerical computation at the design points

case	l_1	l_2	**h**	**combination**	c_l	c_d
1	0.164	0.725	1.843	a2,b2,c2	0.2084	0.6210
2	1.164	1.225	2.5	a2,b1,c1	0.2079	0.5618
3	1.164	0.725	2.5	a2,b2,c1	0.1503	0.5725
4	1.164	1.225	1.843	a2,b3,c3	0.2672	0.5839
5	1.164	0.225	1.843	a2,b3,c3	0.1381	0.6484
6	1.164	0.225	1.843	a2,b3,c2	0.1489	0.6314
7	1.164	0.725	1.843	a2,b2,c3	0.2045	0.6256
8	2.164	1.225	2.5	a1,b1,c1	0.0165	0.4474
9	2.164	1.225	1.184	a1,b1,c3	0.1861	0.4856

10	2.164	0.225	2.5	a1,b3,c1	0.0946	0.4647
11	2.164	0.225	1.184	a1,b3,c3	0.0121	0.5346
12	0.164	0.225	1.184	a3,b3,c3	0.1341	0.6556
13	2.164	1.225	1.843	a1,b1,c2	0.1263	0.4746
14	2.164	0.725	2.5	a1,b2,c1	0.0818	0.5184
15	2.164	0.725	1.843	a1,b2,c2	0.0702	0.5287

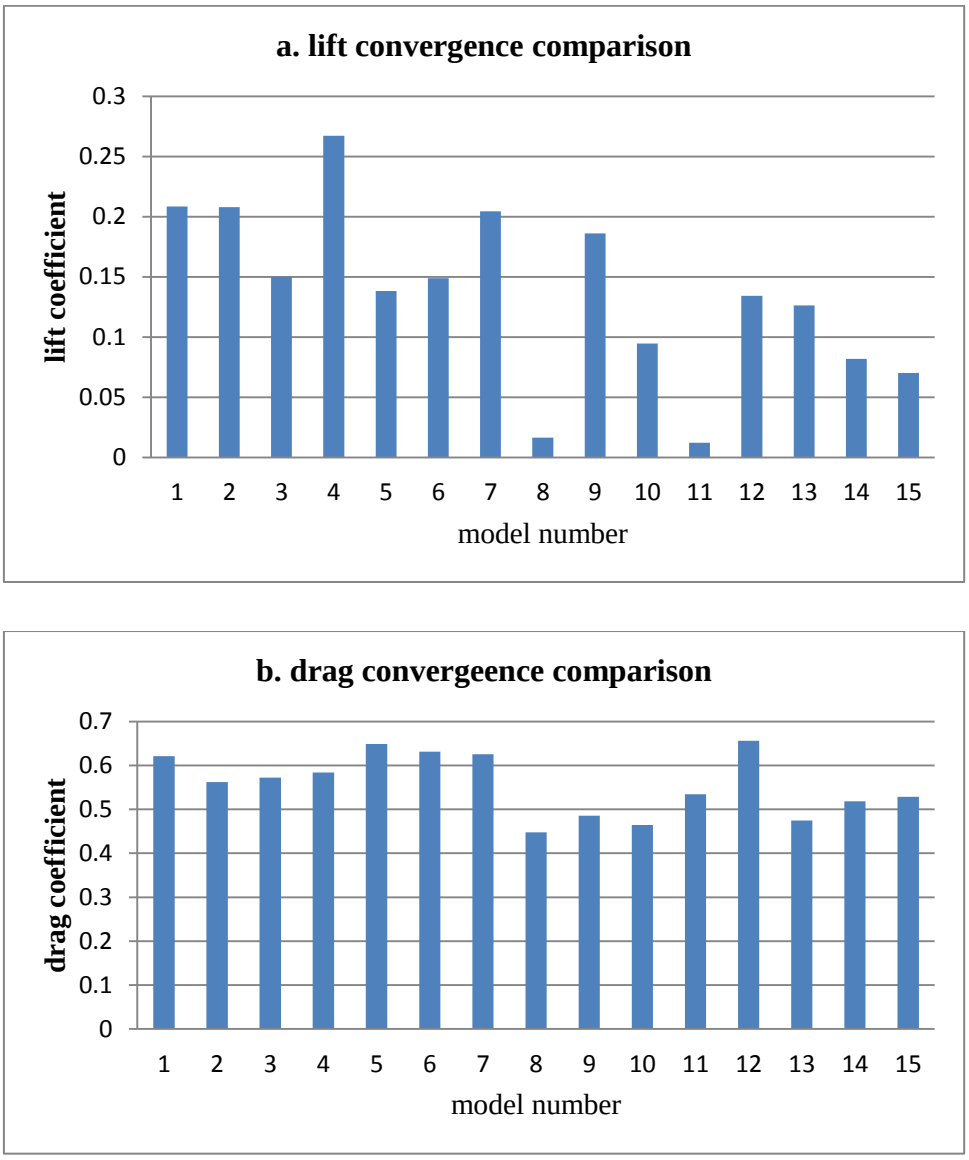

Figure3.9: Drag and lift coefficient comparison plot

3.3.2.4. Adjusting the Concavity and Convexity of the selected model and choosing the better profile

The deformation of the c_1 and c_2 is done using the following equation by fixing the three extreme points. The points in between the three points are changed following the given equation (equation 23) when control point changed by dy_{c1} and dy_{c2}.With this we got four combinations($dy_{c1}dy_{c2;}$-$dy_{c1}dy_{c2;}$-dy_{c2} $dy_{c1;}$-dyc1-dyc2) which create four models again.

By simulating by fluent we chose the better profile with lowest drag coefficient which is the last optimal solution for this paper by choosing $dy = 0.41$we got appropriate spline by using catiaV5.With this, the one formed from $dy_{c1} = 0.41$ and $dy_{c2} = -0.41$have better drag performance. The old and new coordinate points are shown on the following table:

Table 3.3: Deformation of the selected model profile

Point	Original		After optimization		After deformation	
	x	y	x	y	x	y
1	0	0	0	0	0	0
2	90.8	0	107	0	107	0
3	181.6	0	211	0	211	0
4	272.4	0	315	0	315	0
5	363.2	0	419	0	419	0
6	454.192	0	523	0	523	0
7	494.192	16.67	627	0	627	0
8	539.792	82.253	731	0	731	0
9	539.792	269.512	835	0	835	0
10	576.792	397.196	939	0	939	0
11	666.792	605.074	1000	124.463	1000	101.528

12	756.792	810.788	1090.8	309.741	1090.8	249.18
13	846.792	1016.5	1181.6	495.034	1181.6	394.746
14	936.792	1222.22	1272.4	680.339	1272.4	540.87
15	1026.79	1427.93	1363.2	865.658	1363.2	690.286
16	1120.59	1642.33	1454.19	1051.38	1454.19	845.813
17	1164	1843	1494.19	1133.03	1494.19	924.243
18	1120.59	2043.56	1551.5	1250	1551.5	1038.07
19	1026.79	2250.09	1666.79	1485.34	1666.79	1259.32
20	936.792	2448.25	1756.79	1669.04	1756.79	1447.06
21	846.792	2646.42	1846.79	1852.74	1846.79	1643.67
22	756.792	2844.59	1936.79	2036.42	1936.79	1848.29
23	666.792	3042.75	2026.79	2220.08	2026.79	2059.88
24	576.792	3240.92	2093.78	2356.74	2093.78	2232.82
25	539.792	3322.39	2120.59	2411.45	2120.59	2329.63
26	494.192	3422.79	2144	2459.2	2144	2418.94
27	454.192	3509.86	2164	2500	2164	2500
28	363.2	3638.87	2144	2511.86	2144	2551.41
29	272.4	3711.04	2120.59	2525.74	2120.59	2608.05
30	181.6	3754.64	2093.78	2541.64	2093.78	2669.89
31	90.8	3777.53	2026.79	2581.35	2026.79	2760.01
32	0	3783	1936.79	2634.71	1936.79	2868.16
33			1846.79	2688.07	1846.79	2979.19

34			1756.79	2741.43	1756.79	3091.89
35			1666.79	2794.79	1666.79	3204.6
36			1576.79	2848.15	1576.79	3315.24
37			1539.79	2870.08	1539.79	3384.34
38			1494.92	2897.12	1494.92	3451.64
39			1454.19	2920.83	1454.19	3505
40			1363.2	2974.78	1363.2	3582.94
41			1272.4	3028.62	1272.4	3647.78
42			1181.6	3082.45	1181.6	3698.94
43			1082	3141.5	1082	3742.8
44			1000	3190.12	1000	3761.71
45			939	3226.28	939	3755.39
46			835	3287.94	835	3770.07
47			731	3349.6	731	3777.81
48			627	3411.26	627	3780.71
49			523	3472.92	523	3780.64
50			419	3534.58	419	3779.21
51			315	3596.24	315	3777.71
52			211	3657.9	211	3777.12
53			107	3719.56	107	3778.13
54			0	3783	0	3783
	table a		table b		table c	

The original, simplified original and nose profile after shape optimizations are shown on the following figures.

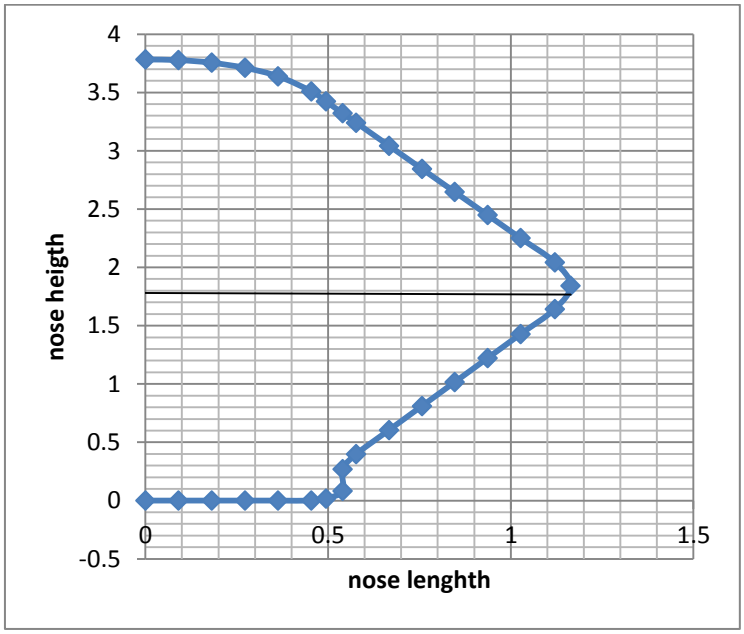

(a) The nose of the original train

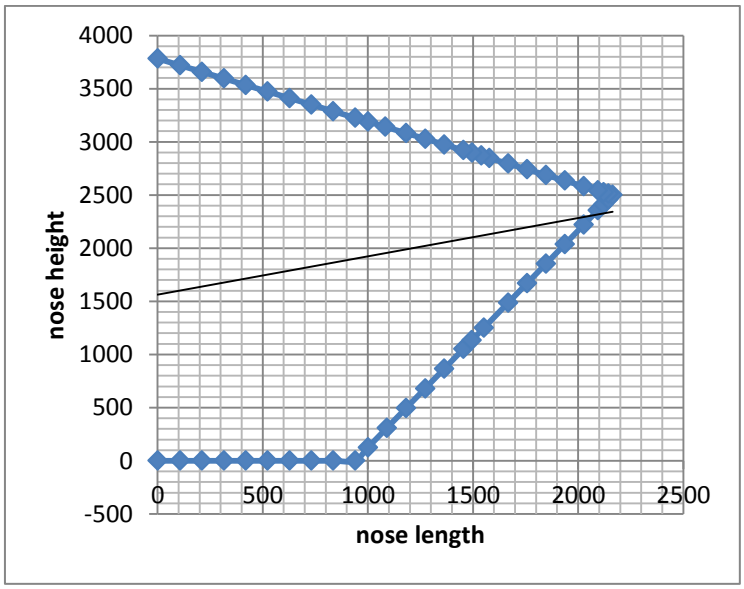

(b) Base nose created for shape optimization

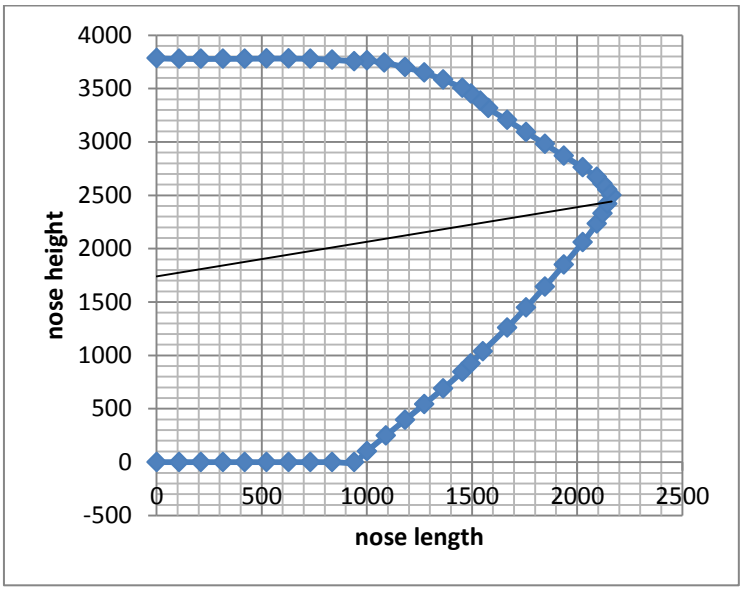

(c) Optimized model train nose

Figure 3.10:2-D Train Nose

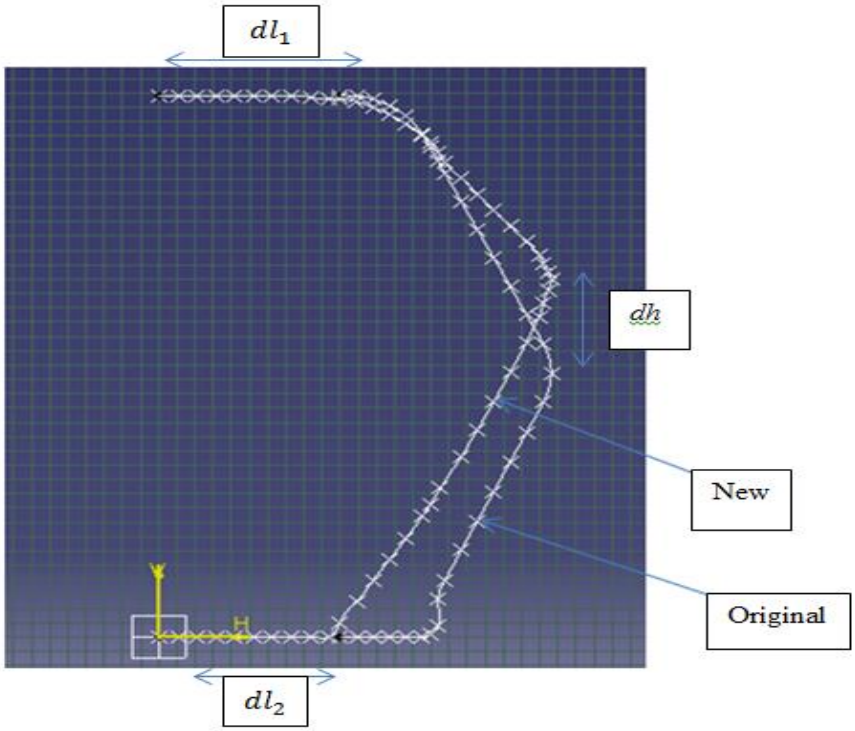

Figure3.11: Points and splines created from excel coordinates on CatiaV5

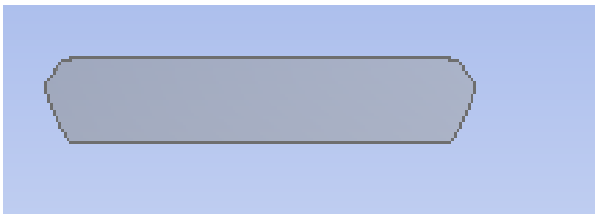

Figure3.12: Optimized model created from the spline

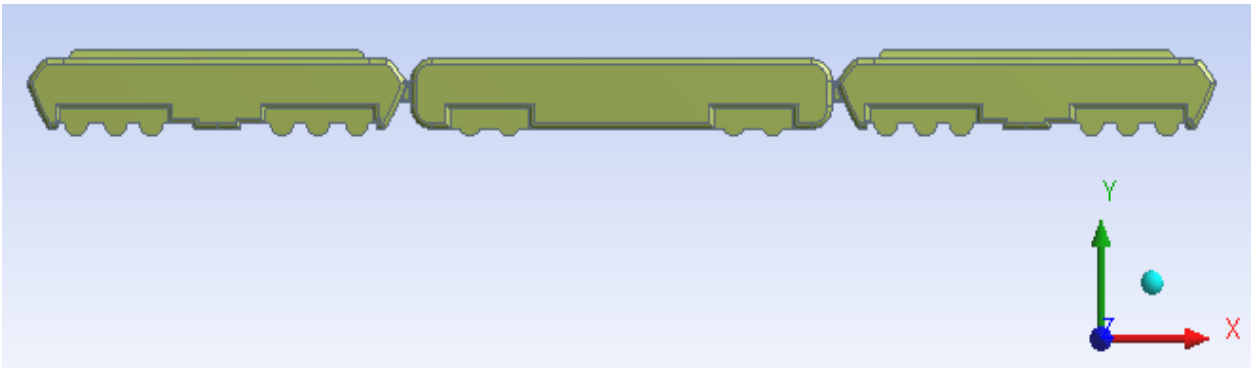

Figure3.13: Optimized ENT

Using the above figure 3.13 the simulation/analysis was conducted using the approach used in the no-cross wind. The result shows that the aerodynamic drag is reduced by 15 percent.

From figure 3.11we can see that by small change on the nose profile we can reduce large amount of drag, without harming the total volume of our train.

3.4. Some Aspects Regarding the Impact of Aerodynamics on Energy (power) Consumption in Railway Applications

The main consequence of an air flow surrounding a moving train resides in the aerodynamic drag and a certain pressure distribution on the frontal and lateral surfaces of the vehicle. The actual value of the aerodynamic drag (if pre-determined) may lead to a more accurate design of the whole locomotive power transmission. The aerodynamic drag may be estimated by using two specific experiments: the traction method and the free launch method. While the first one uses highly sophisticated equipment, the second is easier to use due to the relative low number of devices required. The present work's main goal is to illustrate the importance of aerodynamic design of the railway vehicles, as their performances are influenced by the aerodynamic drag. In order to illustrate the influence of the aerodynamic shape of locomotive body, we have chosen the latest electric model available on our case, the HXD1C locomotives, currently in selection at the national passenger railway.

3.4.1. Introduction to Energy Consumption

It is a general common fact that in the case of any railroad administration, the increment of the speed rates including the one of the diesel traction has led to the development of issues regarding the aerodynamic drag and energy consumption.

The classical formula of the aerodynamic drag of a railway vehicle is known as being a second degree polynomial with the shape $a + bv_t + cv_t{}^2$[21].The formula is known as "the Davis formula" and can be applied to the alignment and plateau traffic. The term a stands for all the mechanical resistances during the motion, generally dependent to the weight per axle. Term bv_t stands for all the other types of non-aerodynamic drags. Usually, term b is splitted in other two terms, $b_1$andb_2; the first stands for the loss of quantity during the motion while the second term stands for the resistances caused by loss of gearing and the ones that depend on the train weight. Regarding the$cv_t{}^2$term, the Davis formula is a provisional one, because it takes into account only the first three terms of a serial progression representing the total resistance.

The aerodynamic drag is expressed through the third term. It becomes obvious the fact that at high speed rates, this term becomes predominant due to the square of the velocity. Due to this reason, one of the possible improvements in aerodynamic drag is to reduce this term as much as it can be reduced. In practice, this fact could be translated by adopting a body shape with a

form and a front surface that would maintain the $c$constant (which takes into account quite all of these aspects) at a minimum value.

In the area of speed rates under 120 km/hr., the term $c{v_t}^2$expresses with adequate accuracy the external aerodynamic drag. The c term can be splitted as follows:

$$c = \frac{1}{2} c_x s \rho \quad \ldots \ldots \ldots \ldots \ldots \ldots \ldots \ldots \ldots \ldots \ldots \ldots \ldots \ldots \ldots \ldots \ldots 24$$

Wherec_x – the coefficient of air penetration (dimensionless); s – the frontal surface of the vehicle: ρ – the density of the air.

Also, there have to be taken into account the following aspects:

- The vehicle (the train) is moving through a non-stationary air mass and the wind may have major influence, including on the alignment and plateau traffic;
- The density probability of the speed of wind follows an approximate Gaussian distribution;

The c_x coefficient can be measured with maximum accuracy in wind tunnels, but correct enough approximations can be also achieved by launching the vehicle on a known slope, only when knowing the other mechanical resistances.

The influence of the wind can be expressed through two correction coefficients, k_w and k_y (both being functions of the speed of train and of the speed and wind direction).

The $k_w$coefficient expresses the relative velocity of the train compared to the one of the air (resulting from the speed of movement and from the speed of the wind). This applies, in the same way, to the b_1 term.

The k_y coefficient expresses the change of the penetration coefficient c_x in case of aerodynamic drag. Another effect on the aerodynamic drag to motion resistance is determined by tunnels. The tunnel effect has been recently carefully studied, especially in the case of high-speed trains. This effect can be expressed through a coefficient, noted still ask_t.

The influences of the gradients and curves are also to be taken into account in order to express the accurate value of the total drag. Thus, by noting the specific aerodynamic drag with r and the specific resistance given by the gradient with **i** respectively r_c for the

specificresistance given by the curve (all expressed in N/kN), the total mechanical and aerodynamic drag of a locomotive may be written as follows [21]:

$$\boldsymbol{R} = rmg = \left[a + (k_w b_1 + b_2)v_t + k_t k_w k_y c_x s\rho * \frac{1}{2}{v_t}^2 \pm \boldsymbol{i} + r_c\right] mg \quad \ldots\ldots\ldots\ldots\ldots\ldots\ldots 25$$

The locomotive has to generate the necessary traction power to mainly overcome its own total mechanical and aerodynamic drag and the rest of the train and after, to allow it to be hauled within the required speed limits. The c factor from the Davis equation has a determining role within this fact, especially during the movement, where it is predominant.

The present study proposes the analysis of one of the most important means of reducing the energy consumption by reducing the c coefficient.

The most important consequence of the existence of a still part of the aerodynamic drag coefficient is the fact that when a train is integrated in rigid consists, or even in double or triple sets it runs faster and spends less energy than when it is integrated in a single configuration.

This reality is reluctant to the theoretical calculus of the motion and consumption, based on the use of the conventional formulas of the aerodynamic drag. Thereafter, the strictly use of the empirical formulas of the aerodynamic drag can generate erroneous results.

3.4.2. The Practical Case Study of AA-DD

In the specific case of our train shapes (as the ones used in Locomotive front profile) there are two coefficients that matter the most:

- The frontal aerodynamic coefficient, c_x
- The lateral aerodynamic coefficient, c_y

When dealing with the calculus of the specific aerodynamic drag, the most important coefficient to be taken into account is the frontal one. Its influence is best illustrated by the following equation:

$$c_x = \int_s^{\cdot} c_p \frac{ds_x}{s_r} = \int_s^{\cdot} \frac{p - p^-}{\frac{1}{2}\dot{\rho}\dot{u}^2} \cdot \frac{ds_x}{s_r} = \frac{\frac{Fx}{1}}{2} \rho \dot{u}^2 s_r \quad \ldots\ldots\ldots\ldots\ldots\ldots\ldots\ldots\ldots\ldots\ldots\ldots\ldots\ldots\ldots\ldots 26$$

$c_x$may be determined theoretically by integrating the pressure coefficient, c_p. In the equation above F_x – the total effective force to which the body is subjected to; u - the average fluid speed [m/s]; s_r – the reference surface [m^2]; ρ – the fluid density [kg/m^3].

$$c_y = \int_s^{\cdot} c_p \frac{ds_y}{s_r} = \frac{\frac{Fy}{1}}{2} \rho \mathring{u}^2 s_r \quad \ldots\ldots\ldots\ldots\ldots\ldots\ldots\ldots\ldots\ldots\ldots\ldots\ldots\ldots\ldots\ldots\ldots\ldots\ldots\ldots\ldots\ldots\ldots\ldots\ldots\ldots\ldots\ldots 27$$

For the lateral parts of the vehicle the appropriate coefficient,c_y will be calculated in a similar manner. Thus, The mechanical labor of the traction forces for a locomotive hauling a train with the total mass m on the $\Delta S = S - S0$ distancemay be written as:

$$L_{01} = \int_{s0}^{s} F_0 ds \quad \ldots\ldots\ldots\ldots\ldots\ldots\ldots\ldots\ldots\ldots\ldots\ldots\ldots\ldots\ldots\ldots\ldots\ldots\ldots\ldots\ldots\ldots\ldots\ldots\ldots\ldots\ldots\ldots\ldots\ldots\ldots\ldots 28$$

Where

$$F_0 = \acute{m} f_0 = \mathrm{m}\left(\frac{1}{\beta}\frac{\mathrm{dv}}{\mathrm{dt}} + r_t \pm i + r_c + f_f\right) \ldots\ldots\ldots\ldots\ldots\ldots\ldots\ldots\ldots\ldots\ldots\ldots\ldots\ldots\ldots\ldots\ldots\ldots\ldots\ldots\ldots\ldots\ldots\ldots 29$$

, stands for the traction force produced by the locomotive

The specific mechanical drag of the locomotive is

$$r_t = a + (k_w b_1 + b_2) v_t + k_t k_w k_y c_x s \rho * \frac{1}{2} {v_t}^2 \pm i + r_c + f_f \quad \ldots\ldots\ldots\ldots\ldots\ldots\ldots\ldots\ldots\ldots 30$$

In this case, the total necessary traction force will be:

$$F_0 = \acute{m}\left(\frac{1}{\beta}\frac{\mathrm{dv}}{\mathrm{dt}} + \mathrm{a} + (k_w b_1 + b_2) v_t + k_t k_w k_y c_x \mathrm{s} \rho * \frac{1}{2} {v_t}^2 + r_v \pm i + r_c + f_f\right) \ldots\ldots\ldots\ldots\ldots\ldots\ldots\ldots\ldots\ldots\ldots\ldots\ldots\ldots\ldots\ldots\ldots\ldots\ldots\ldots\ldots\ldots\ldots\ldots 31$$

3.4.3. The Influence of c_x on Energy Consumption

The HXD1C class locomotive's actual body shape has very poor aerodynamics due to the large frontal surface and sharp edges on every corner (see the figure of the HDX1C). The main goal of this study is to demonstrate that a non-aerodynamic vehicle body may influence the energy consumption, especially at high speeds. The simulation or determination of the influence of c_x on energy consumption can be done by imposing more conditions, such as:

- The alignment and plateau traffic at a constant speed (120 km/hr.);
- Traffic within the curve etc.

- The variation of the coefficient is influenced by the following factors:
- Shape and size of the frontal surface of the locomotive;
- The pressure variations on the frontal surface;
- The additional aerodynamic strains.

After the experimental analysis, for the new streamlined form of the car body there have been achieved lower values of strains at the level of the frontal surface. When dealing with the calculus of the specific aerodynamic drag, the most important coefficient is the frontal one. The size of the frontal surface or projected area of the locomotive and its assemblies are approximately 12.468 m^2.Under these conditions the value of the c_x coefficient is approximately around 0.93.

In order to reduce the aerodynamic drag some practical measures have been taken (e.g. reduce the frontal surface or increase the angle of the frontal body in order to reduce the full frontal impact force and pressure. Figure 3.12 presents a new and improved aerodynamic shape, with rounded edges and perfectly smooth at the upper side of the body, so that all possible discontinuities have been removed.

All simulations are done using special FEA software, ANSYS fluent 3D Fluid. As the simulations proved, the main aerodynamic stresses occur at the upper side of the body, due to the sharp edges and the aerodynamic shock induced by the air conditioning unit and other accessories which is placed right above the driver's cab. The situation is obvious for both, the frontal air flow and lateral wind as well.

Due to this, the new c_x resulted as 0.79, which is 15% lower than the initial one and much closer to the lower limit of 0.5, which is considered to be the best in case of the rail vehicles

[21]. Consequently, the entire aerodynamic drag was reduced by 15% (other factors are negligible) and thus, energy consumption under these specific conditions may be reduced. It is important to highlight that energy consumption in railway applications is a very complex issue and aerodynamic drag has its influence but only at high speeds.

At high speed the aerodynamic resistance dominates mechanical and other non-aerodynamic resistance. Which means the significance of $a + (k_w b_1 + b_2)v_t$ is low. Also at flat traffic we can leave the effect of gradient resistance ($\pm i$) too. When there is no curve and low friction value also have little effect compared to the effect of aerodynamic resistance at high speed. In this case the value of $c_y << c_x$ which gives c_x approximately equal to c_d.

This gives us the equation:

$$r_t = k_t k_w k_y c_x s\rho * \frac{1}{2} {v_t}^2 \qquad \text{...} 32$$

As specified in the above discussion we have high frontal drag coefficient of around 0.93 before shape optimization which dominates lateral drag and was equal to c_x.After shape optimization was done drag coefficient of around 0.79 was found. From this we have calculated decrease in drag coefficient as:

$$\frac{(0.93 - 0.79)}{0.93} * 100\% = 15\%$$

This decrease in drag coefficient will decrease the aerodynamic resistance with the same factor. This definitely will result in the decrease in energy consumption. So by improving the aerodynamic performance of the train we can improve energy consumption.

CHAPTER FOUR: RESULTS AND DISCUSSIONS

4.1. Aerodynamic Simulation of the Train

4.1.1. Aerodynamic Simulation of the Train With-out the effect of Cross-wind ($\alpha = 0$) at 120 km/hr (34m/s)

Using k-epsilon, realizable, non-equilibrium wall function method the following result was achieved.

The solution is converged at 782'siteration; the drag coefficient is 0.93 and the lift coefficient is 0.1775.the resulting aerodynamic parameters are listed in the following section. The moment coefficient convergence history and pressure contour also listed below. The moment coefficient at the length at lower floor of the train is 6.8. From the result below we can see that the drag coefficient is very high compared to recommend lowest $c_d$valuewhich is 0.5 for best design profile in high speed train [21].According to the paper by Ioan SEBEŞAN and Bogdan TARUS [21] done on regional train the recommended lowest value of drag coefficient is 0.5 which is close to the result he found (0.54).In our case the locomotive used is freight locomotive which poor in air penetration. Hence the frontal shape of our train is almost rectangular the result (0.93) would make sense. As discussed in the previous section of this paper the main objective of this study is to reduce this value as much as possible. The value for c_l is much lower than $c_d$which is in recommended area. The highest value of the drag pressure is 784pa which is around extreme point of the front area of the nose which requires shape optimization. The result gained after the shape optimization is listed in the next discussion.

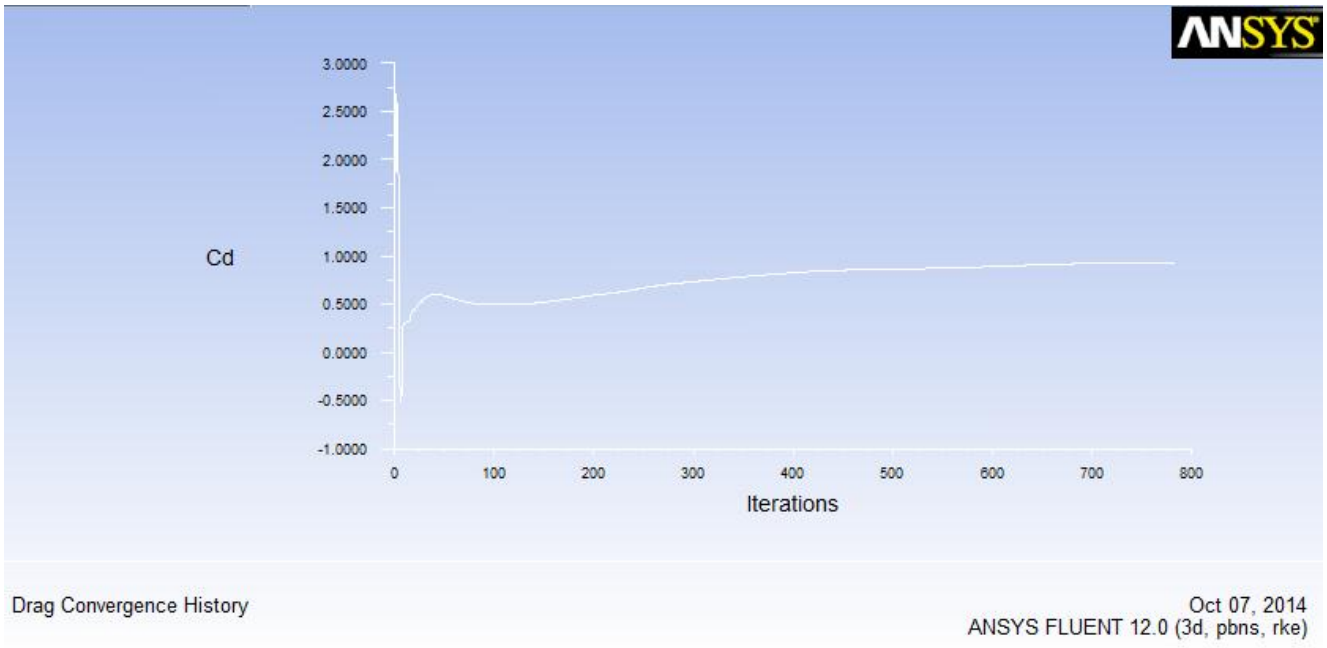

(a) Drag convergence history

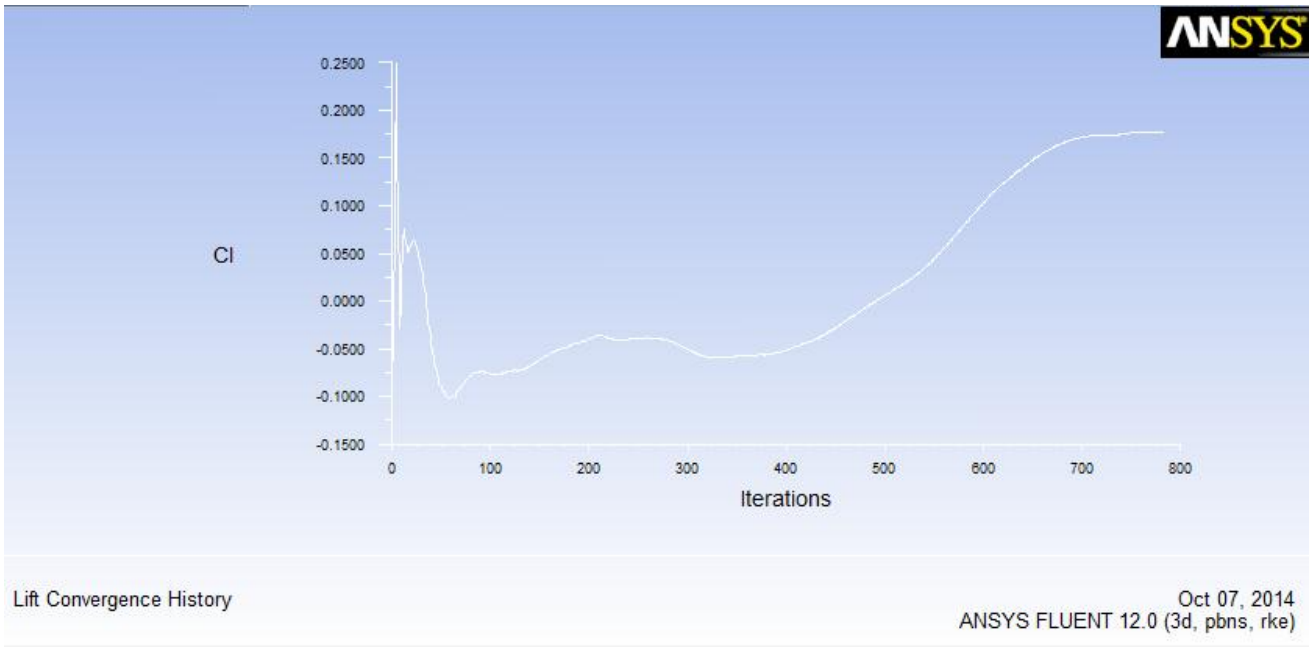

(b) Lift convergence history

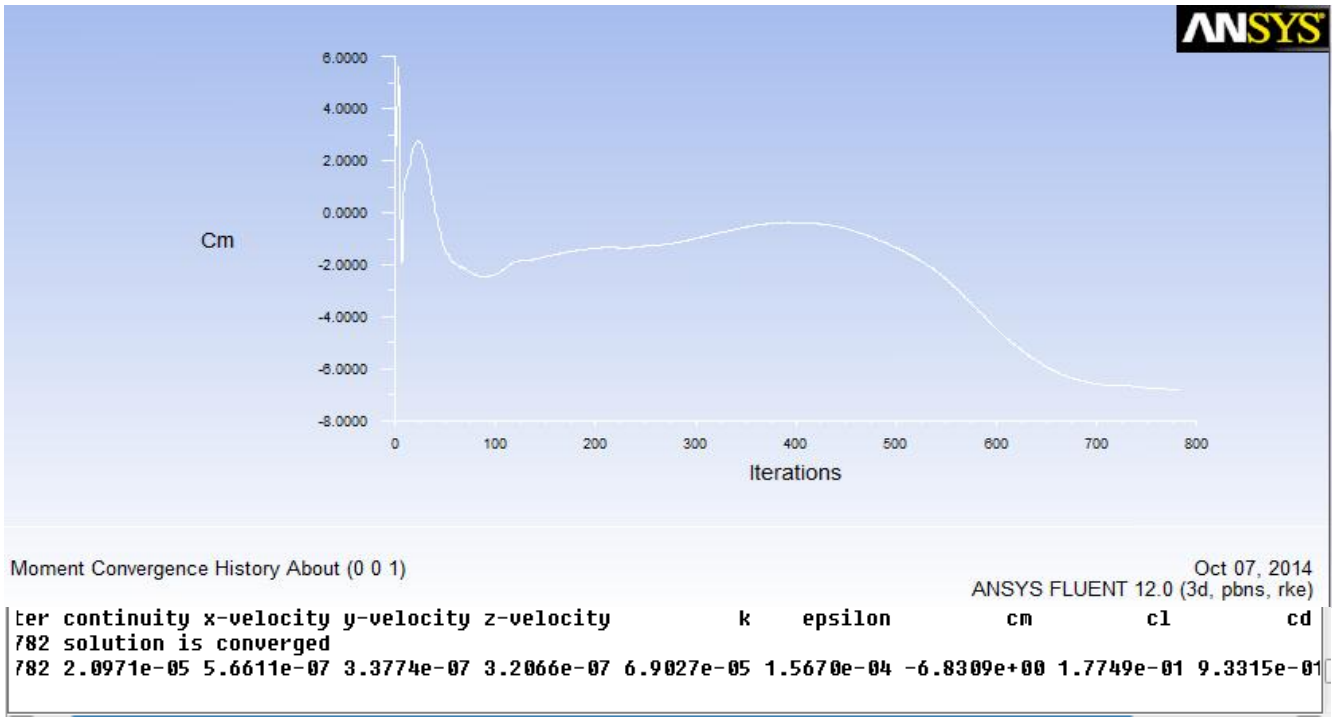

(c) Moment convergence history

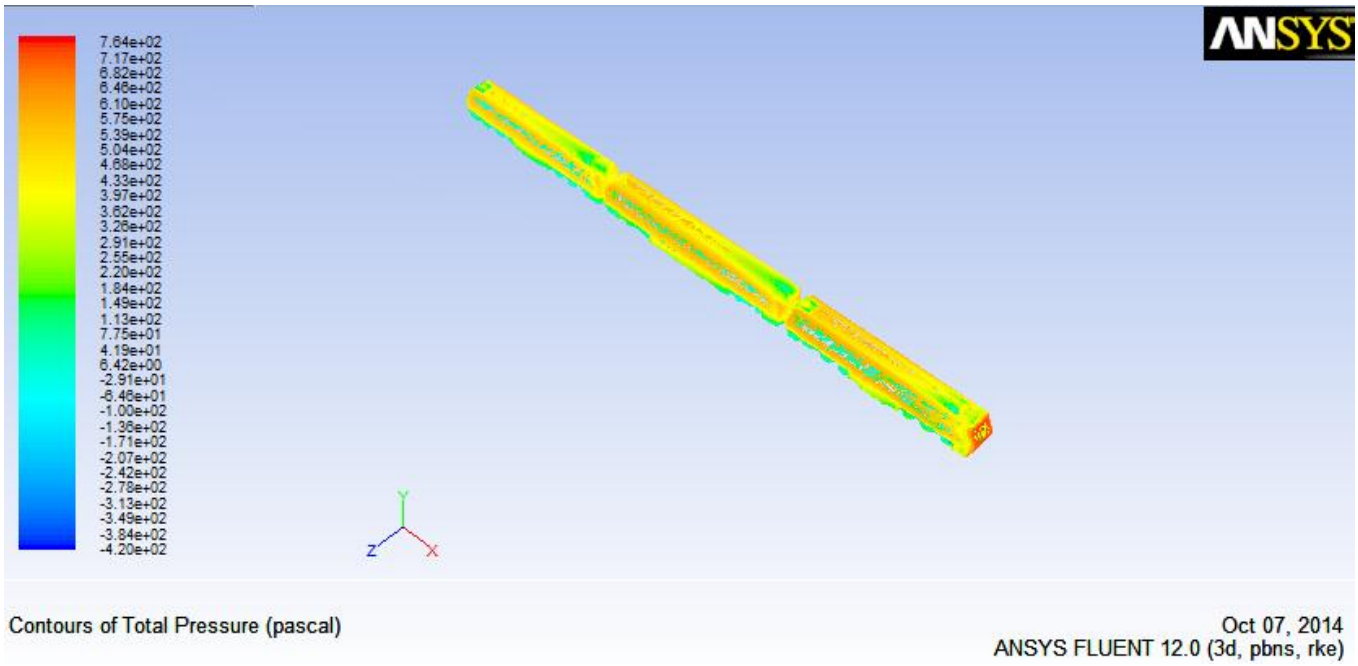

(d) Total pressure contour

Figure4.1: The aerodynamic characteristics of ENT at 120 km/hr. without cross-wind effect

4.1.2. Aerodynamic Simulation of the Train with the effect of Cross-wind ($\alpha \neq 0$) at 120 km/hr (34m/s)

Result shows that as the degree of rotation increase all the aerodynamic characteristics increase in significant way. Because of this even though the train is low speed train care must be taken especially when there is strong cross wind and at curvature or embankment.

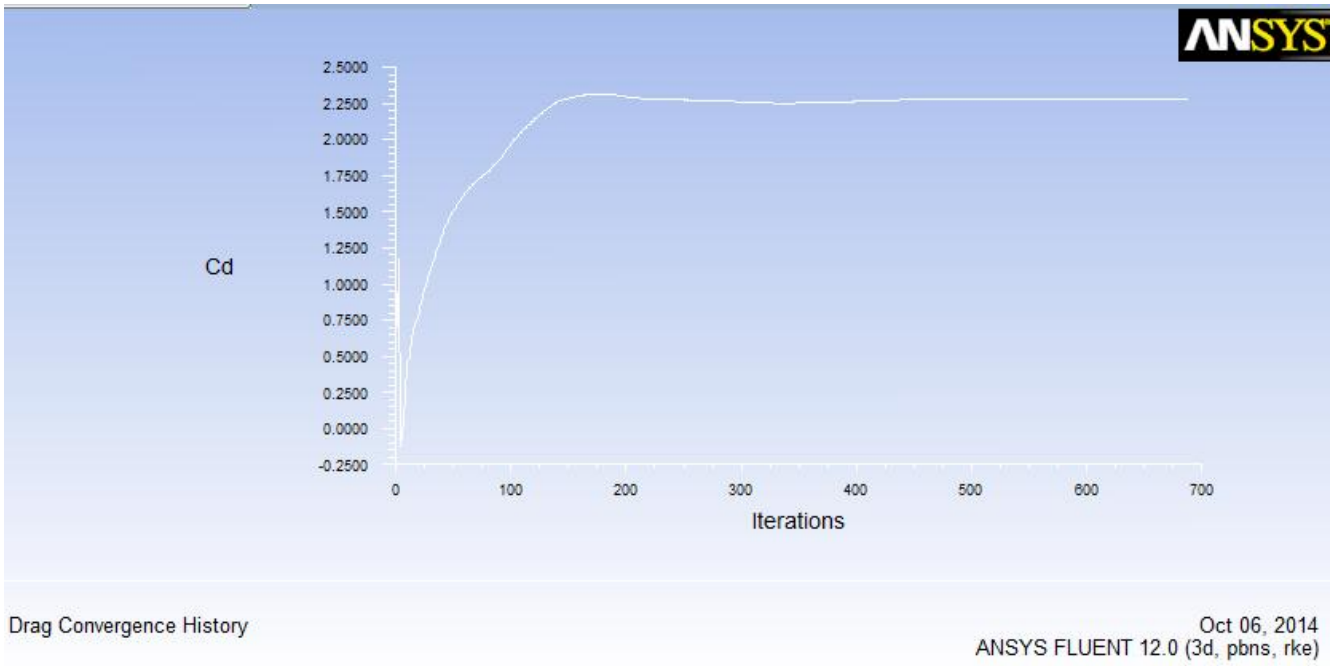

(a) Drag convergence history

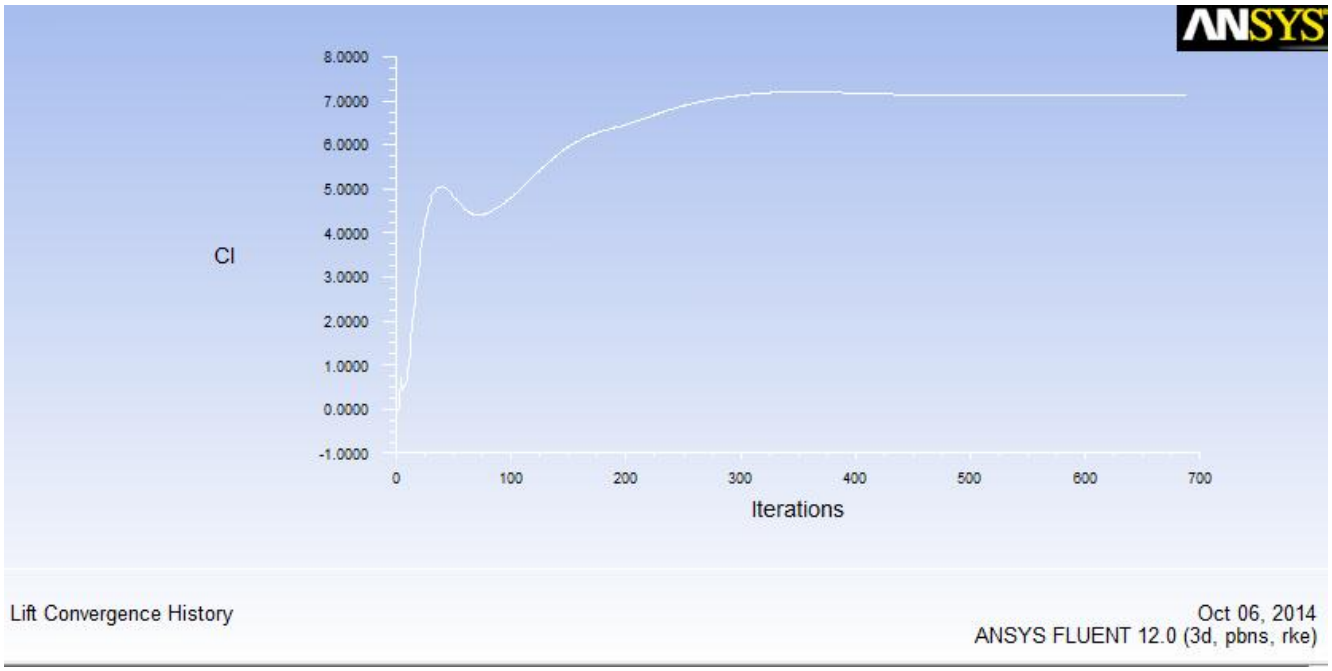

(b) Lift convergence history

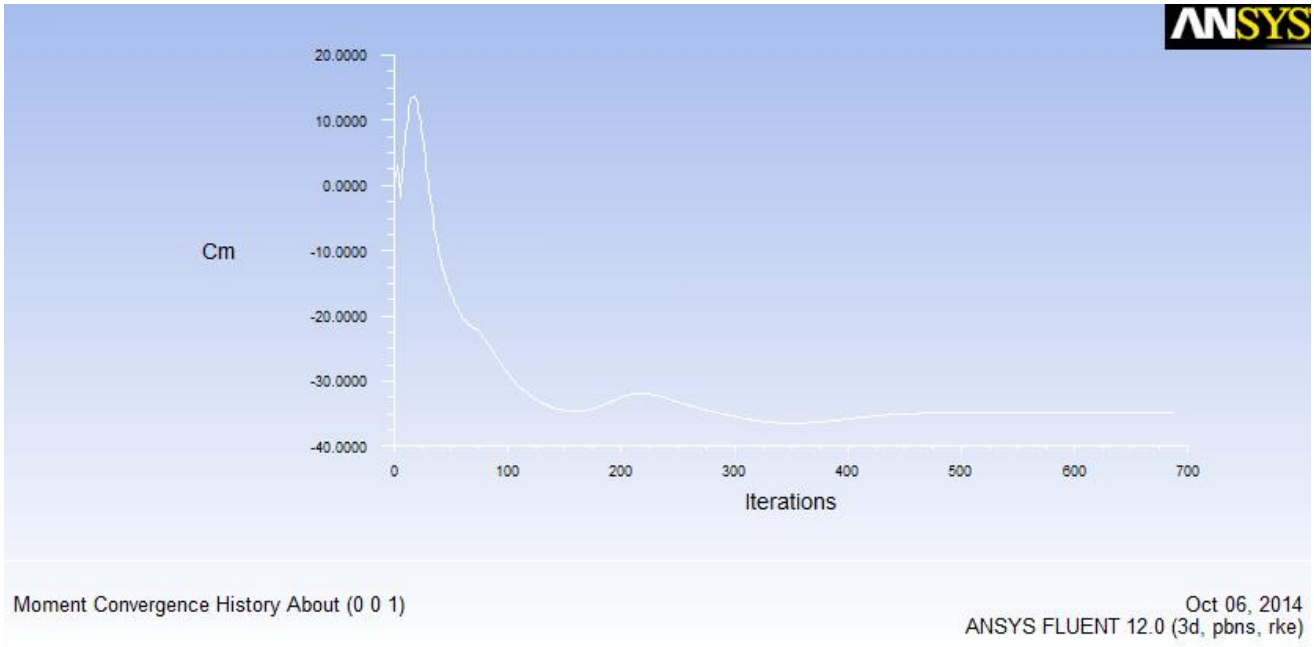

(c) Moment convergence history

(i) At $\alpha = 30$

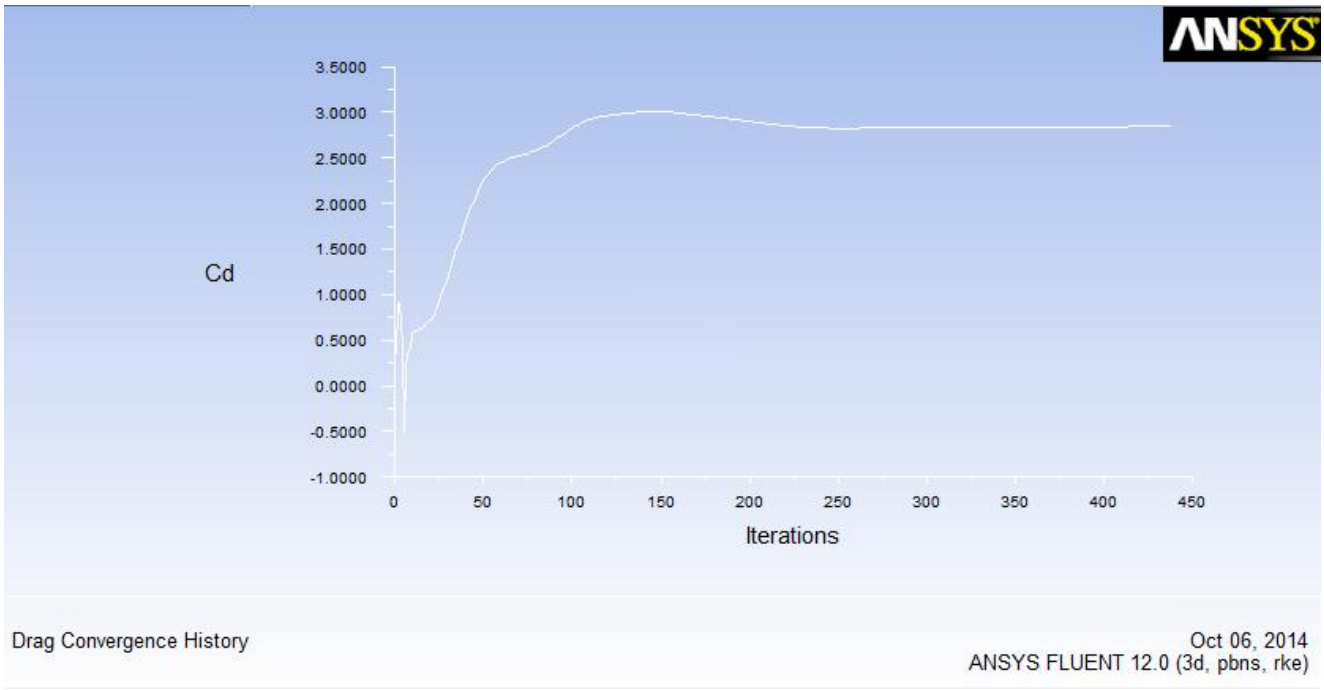

(a) Drag convergence history

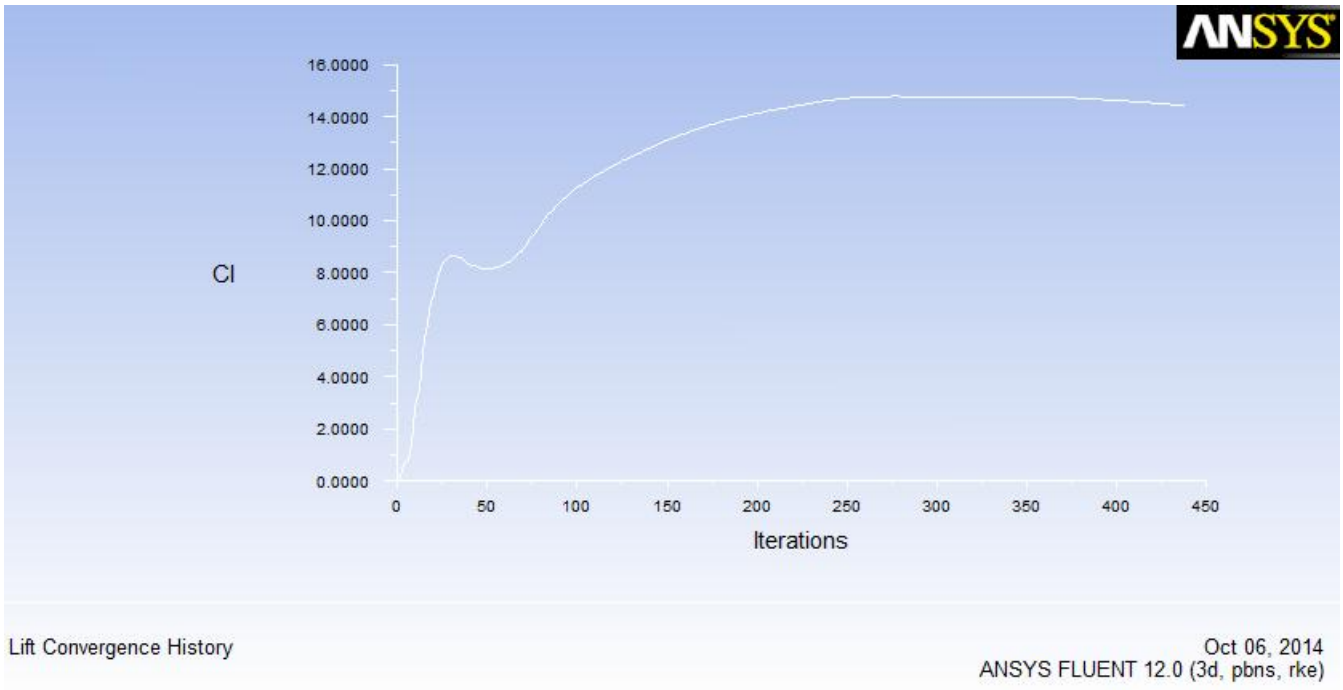

(b) Lift convergence history

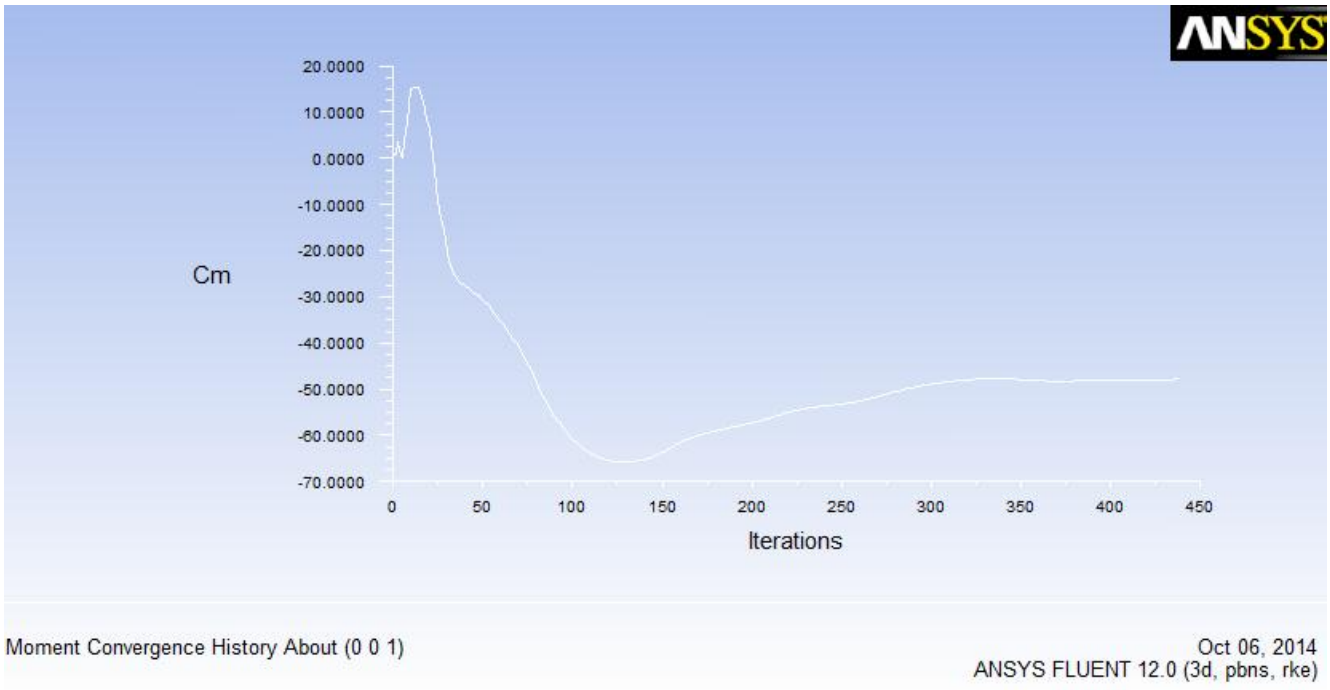

(c) Moment convergence history

(ii) At $\alpha = 45$

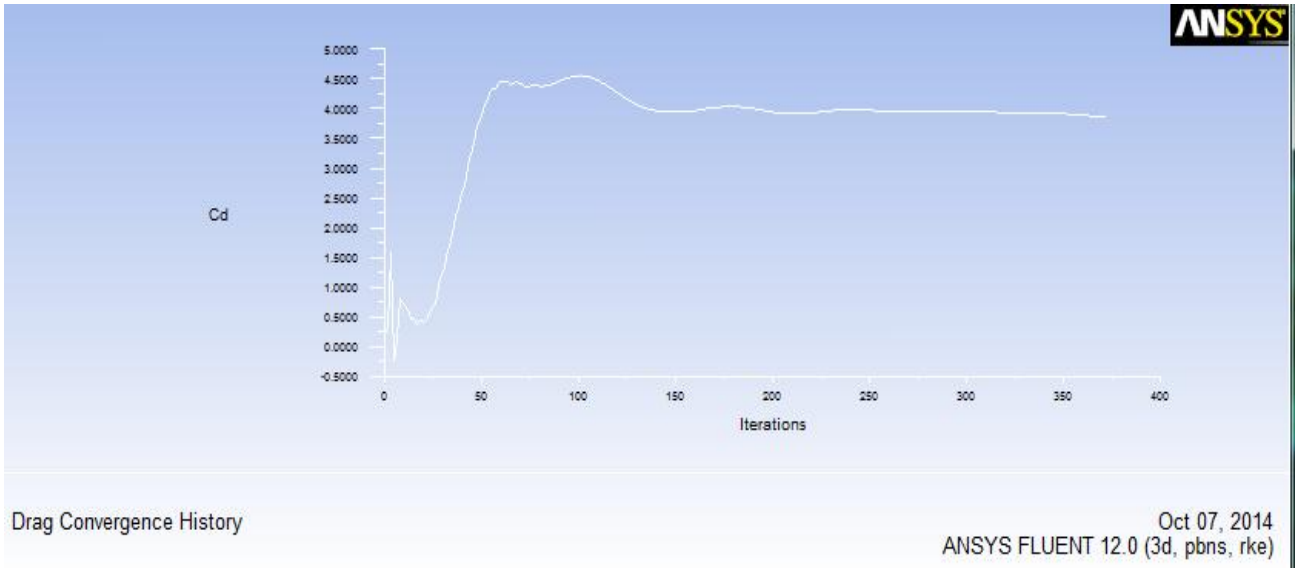

(a) Drag convergence history

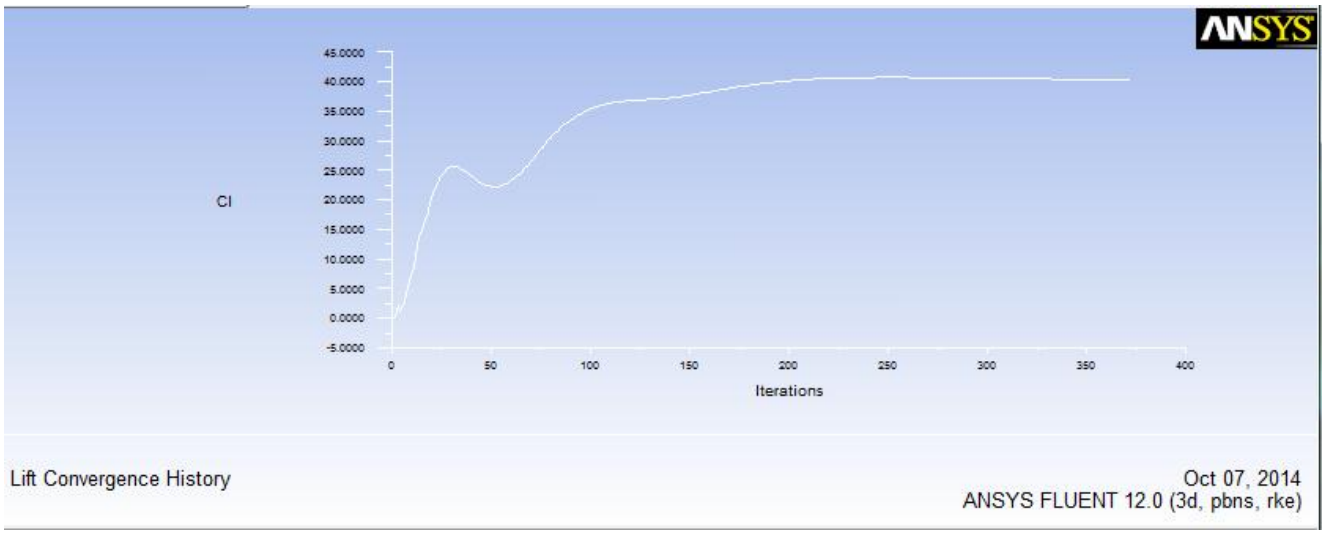

(b) Lift convergence history

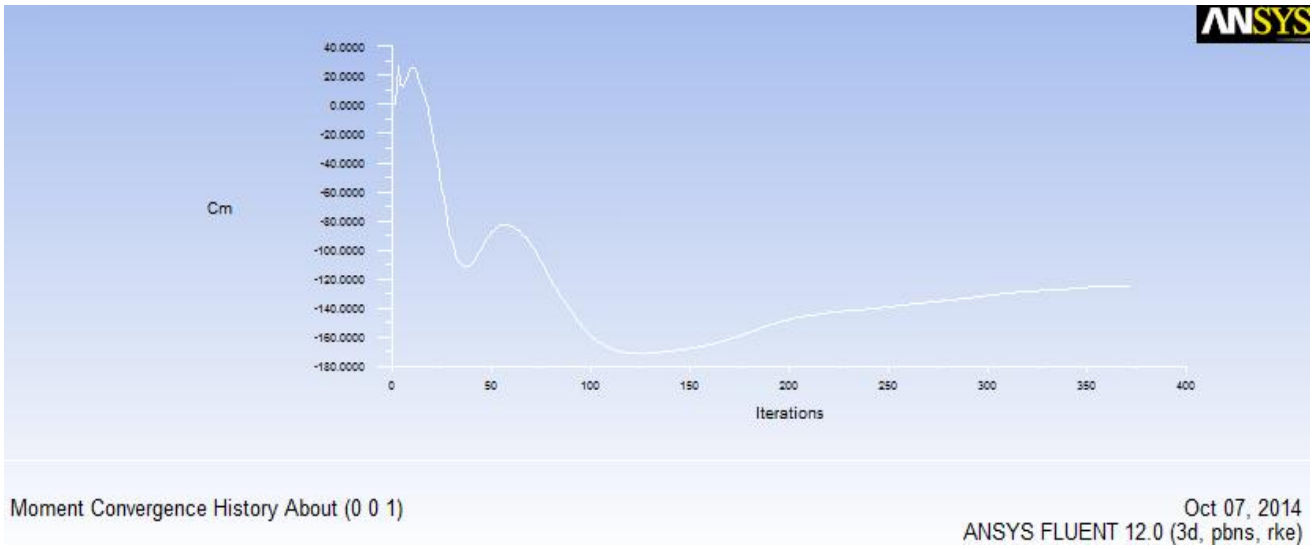

(c) Moment convergence history

(iii) At $\alpha = 60$

Figure4.2: The aerodynamic characteristics of ENT at 120 km/hr. with cross-wind effect

4.2. Aerodynamic Simulation of the Optimized Train Without the effect of Cross-wind ($\alpha = 0$)

After the shape optimization is done the result was achieved using the same computation method. The coefficient of drag is 0.79which is 15% less than the original one. The value of lift coefficient is 0.064, moment coefficient 4.046 and maximum total pressure is around 789.Also there an increment in the others the value of drag coefficient is reduced much which is our main goal. The increment in the other values is not that much significant they are within recommended range. These results indicate that without affecting the carrying capacity (volume) of the train with little modification we can safe lots of energy by reducing drag coefficient which is directly related to energy efficiency. However the structural perspective of the design also needs to be carried out.

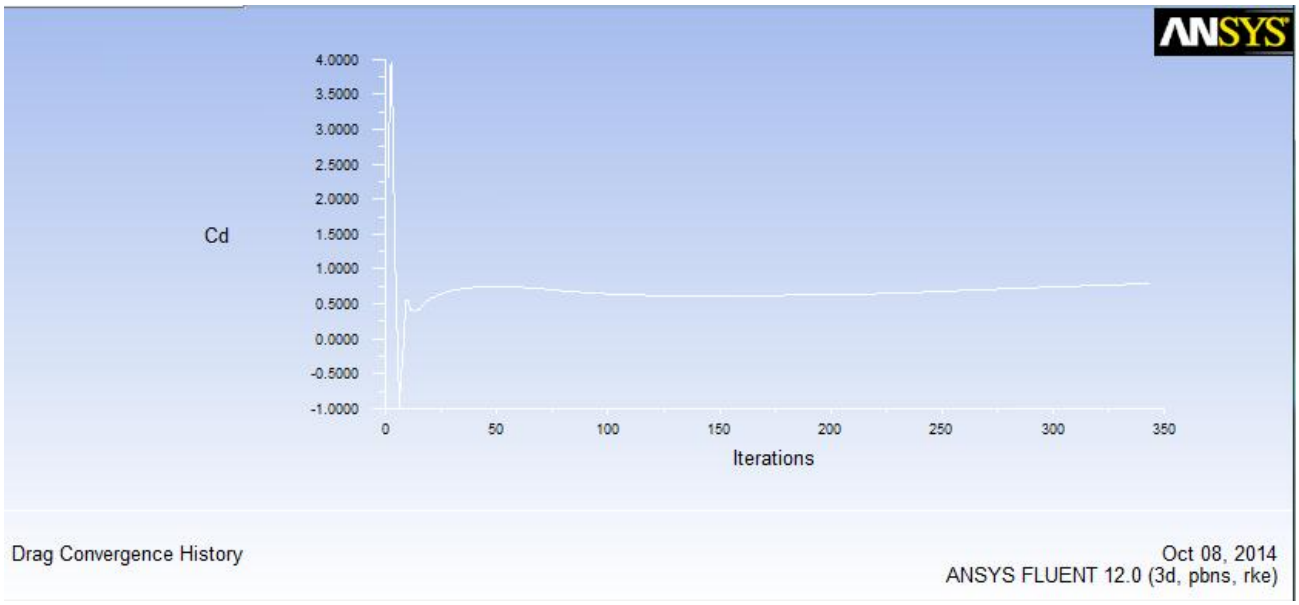

(a) Drag convergence history

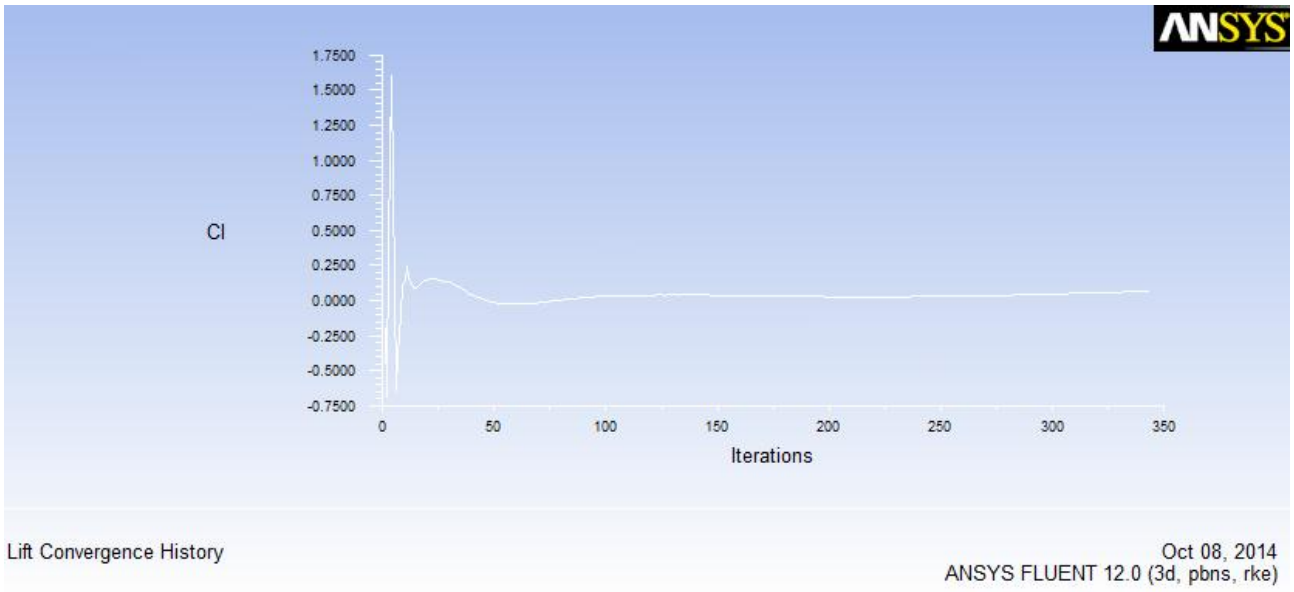

(b) Lift convergence history

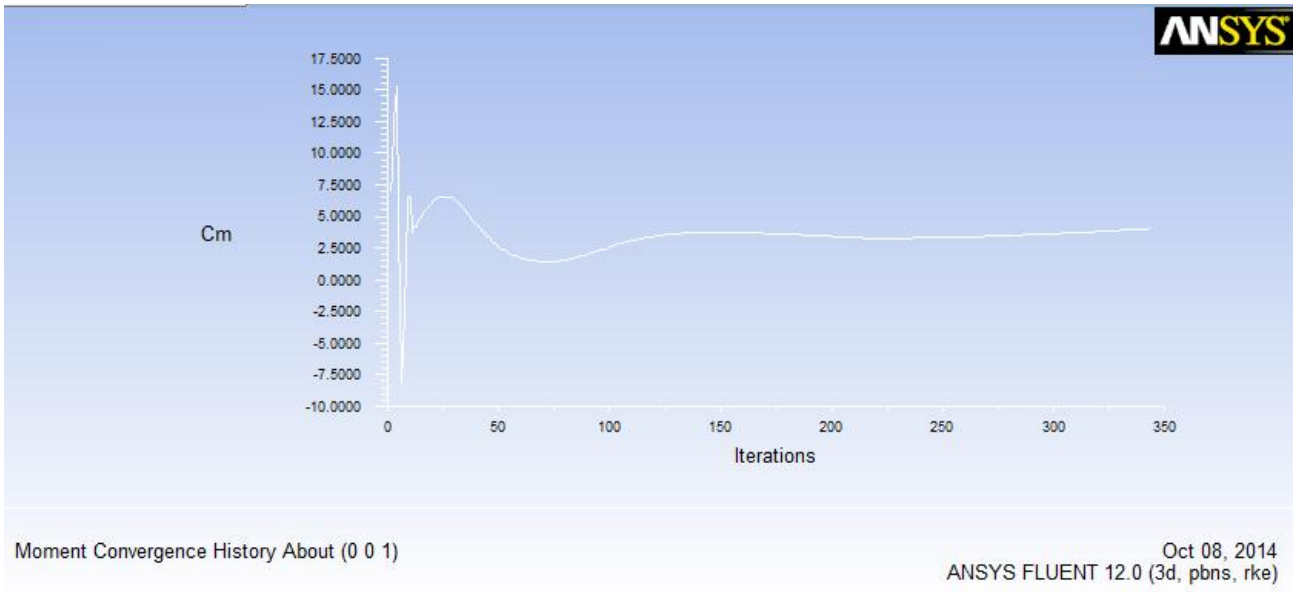

(c) Moment convergence history

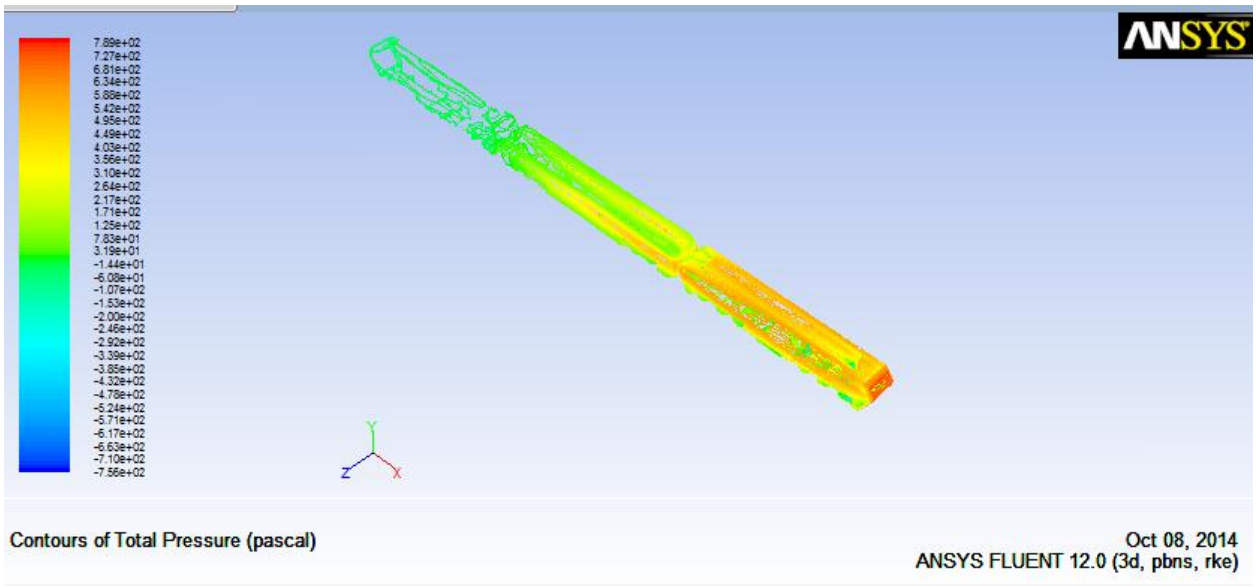

(e) Total pressure contour

Figure4.3: The aerodynamic characteristics of Optimized ENT Without cross-wind effect

CHAPTER FIVE: CONCLUSION, RECOMMENDATION AND FUTURE WORK

5.1. Conclusion and Recommendation

In this thesis Ethiopian National train (ENT) specifically Addis Ababa to Dire Dawa Passenger Train's aerodynamic characteristics, cross wind stability checking, shape optimization and fuel consumption aspect are studied. For the study computational fluid dynamic simulation using ANSYS fluent 12.0 by steady RANS method is used to determine the aerodynamic performance and cross wind stability of the train. For shape optimization of the train head multi-objective approximation method integrated with response surface methodology was used. Energy consumption perspective was discussed using relation between fuel and frontal aerodynamic drag reduction.

- From the study the following conclusion is figured out:
  - The train has poor aerodynamic performance because of its frontal shape.
  - Care must be taken on the curves, embankment and when there is strong cross wind because of low performance of the train against cross wind.
  - By small change to the front profile and length of the train head it was possible to reduce drag coefficient of the train; as the train head is the area with higher pressure receiving zone.
  - By the reduction of the drag coefficient we can improve the energy efficiency of the train.
- By using transient RANS method we can improve the result even though its time consuming requires large capacity computes.

5.2. Future Work

This study is used for some original head shape, often required to improve the aerodynamic performance (drag coefficient, lift coefficient, etc.), to reduce the energy consumption and improve the operational safety of the train. It focuses on the 2-D parameterization of train head. But for better shape profile it has to be 3-D parameterization. In addition to head profile parameterization the method used to find optimized variables mat lab Inc. need to be used for better result. By changing parameterization method this paper can be extended and will be used in high speed train shape optimization. This can be done following the steps: The 3D parametric model of the train is established by CATIA. To achieve the automatic deformation of the head shape, the following three tasks need to be done successively:

1. Establish the entity model of the left half of a train head;
2. Describe the train head by spline surface created from spline curve which consists of selected n control points.
3. Parameterize the left half of the train head using the script file of CATIA;
4. The coordinates of n control points of the left half portion can be recorded automatically to the script file by CATIA, and then the deformation of the head shape can be achieved by modifying the coordinates of n control points.
5. Modify the parameter values in the script file of CATIA using a MATLAB program, and perform the deformation of the train head by running the script file.

To optimize the head shape of the train, five optimization design variables are selected, which correspond to the longitudinal symmetry line, the maximum horizontal contour line, the bottom horizontal contour line, the central auxiliary control line, and the nose height, respectively. With the increase of the streamlined length, the aerodynamic performance of the train will significantly be improved. Therefore, on the basis of a fixed streamlined length, the external shape of the train head is optimized to improve the aerodynamic performance and vehicle dynamic performance of the train. When optimization design variables are determined, the coordinates of the n control points in the script file of CATIA are modified by the MATLAB program, and then a new head shape of the train can be produced by running the script file. In this way better result can be achieve.

References

1. T. A. Stolarski, Brunel University Middlesex, UK; Y. Nakasone and S. Yoshimoto, Tokyo University of Science, Tokyo, Japan, 'Engineering Analysis With ANSYS Software', 2006
2. Barnard, George and Hucho, 'History of Vehicle Aerodynamics '.1996, 1997 and 1998 respectively.
3. Florian Guillou, 'CFD Study of the Flow around a High-Speed Train'. Kungliga Tekniska Hogskolan, Stockholm, 2007
4. Erik Bergh, Anna Lind, Oscar Linde and Elin Stenmark: 'Large eddy Simulations on simplified freight train geometries'. Thesis in Fluid Dynamics, Chalmers University of Technology, 2011
5. Dr. Marc Ratzel, 'Streamlining Aerodynamic CFD Analysis'. Altair Engineering, June 2013
6. Surojit Ganguli: 'Numerical Computation of fluid flow'. 10th Indo-German Winter Academy Dec 11-17, Delhi
7. Momtchil Petkov and Mario Roman: 'CFD Training Manual'. University of Connecticut, 2011
8. Dr. Marc Ratzel, 'Streamlining Aerodynamic CFD Analysis'. Altair Engineering, 2013
9. O. Lewis, 'Aerodynamic analysis of a 2-man bobsleigh'. Delft University of technology, 2006
10. M. Ghil and S. Childress, 'Topics in geophysical fluid dynamics: atmospheric dynamics, dynamo theory, and climate dynamics, vol. 60 of applied mathematical sciences'. Springer-Verlag, New York, 1987.
11. Sadraey M. and VDM Verlag Dr. Müller,'Drag Force and Drag Coefficient', 2009
12. D. Ramasamy, K. Kadirgama, A. K. Amirruddin and M. Y. Taib, 'A Vehicle Body Drags Analysis using Computational Fluid Dynamics'. University Malaysia Pahang, 2013
13. Tian Hong-qi: 'Formation mechanism of aerodynamic drag of high-speed train and some reduction measures'. Central South University, Changsha 410075, China, 2009
14. Andrés F. Tabares, Natalia Gómez, César Nieto and Mauricio Giraldo, 'Critical Sources of Aerodynamic Resistance in a Medium Distance Urban Train: a CFD approach'. Universidad de San Buenaventura, Cali – Colombia, 2011
15. Osth, J. and Krajnovic S., 'Simulations of flow around a simplified train model with a drag reducing device'. Proceedings from Conference on Modeling fluid flow CMFF'12 , Budapest, 2012
16. Chris Baker, 'The flow around High Speed Trains'. University of Birmingham, 2008

17. Asress Mulugeta Biadgo, Addis Ababa University; Aleksandar Simonovic, Jelena Svorcan and Slobodan Stupar, University of Belgrade 'Aerodynamic Characteristics of High Speed Train under Turbulent Cross Winds: a Numerical Investigation using Unsteady-RANS Method'. Belgrade, 2013
18. VeeraVenkata Sunil Kumar Vytla, 'Multidisciplinary Optimization Framework for High Speed Train using Robust Hybrid GA-PSO Algorithm'. Wright State University, 2011
19. Sinisa Krajnovic, 'Aerodynamic optimization of vehicles using computational fluid dynamics and response surface methodology'. Chalmers University of Technology, Sweden, 2007
20. Meng-ge Yu, Ji-ye Zhang, Wei-hua Zhang, 'Multi-objective optimization design method of the high-speed train head'. Southwest Jiaotong University, China, 2013
21. Ioan Sebeşan and BogdanTarus, 'Some Aspects Regarding the Impact of Aerodynamics on Fuel Consumption in Railway Applications'. U.P.B. Sci. Bull., Series D, Vol. 73, Iss. 24, 2011
22. Dr. Marc Ratzel and Thomas Ludescher, 'Streamlining Aerodynamic CFD Analyses'. Altair Engineering Inc., USA, 2013
23. Nor Elyana Ahmad, Essam Abo-Serie and Adrian Gaylard, 'Mesh Optimization for Ground Vehicle Aerodynamics'. Coventry University, UK, 2010
24. Alexander Orellano and Martin Schober, 'Aerodynamic Performance of a Typical High-Speed Train'. Center of Competence for Aerodynamics and Thermodynamics Bombardier, 2006
25. Marco Lanfrit: 'Best Practice Guidelines for handling automotive external aerodynamics with FLUENT'. 64295 Darmstadt/Germany, 2005
26. YAO ShuanBao1, GUO DiLong1, SUN ZhenXu1, YANG GuoWei1 & CHEN DaWei2, 'Multi-objective optimization of the streamlined head of high-speed trains based on the Kriging model'. Chinese Academy of Sciences, 2012
27. ANSYS FLUENT 12.0 Tutorial Guide,2009
28. Jean-Luc Peters, 'How to Reduce the Cross Wind Sensitivity of Trains'. Siemens Transportation Systems, Krauss-Maffei Str. 2, 80997 Muenchen, Germany
29. Ben Diedrichs, 'Aerodynamic calculations of Crosswind Stability of a High-Speed train using Control Volumes of Arbitrary Polyhedral Shape'. Bombardier Transportation. Department of Aero- and Thermodynamics, 2008

30. Zhengzheng Yan, Rongliang Chen, Yubo Zhao and Xiao-Chuancai, 'A Scalable Numerical Method for Simulating Flows Around High-Speed Train under Crosswind Conditions'. Shenzhen Institutes of Advanced Technology, 2013
31. Proceedings of: ME2000, 'High-speed Passenger and Intercity train Aerodynamic Computer Modeling'. The 2000 International Mechanical Engineering Congress & Exposition November 5-10, 2000, Orlando, Florida
32. K. Gemba, 'Shape effects on drag'. California State University, May 17, 2007
33. , 'Study of Drag Coefficient using CFD tools'. National Institute of Technology, Rourkela-769008
34. Osama Abdul Ghani, 'Design optimization of aerodynamic drag at the rear of generic passenger cars using NURBS representation'. University of Ontario Institute of Technology, 2013
35. V. V. Vytla, P. G. Huangy and R. C. Penmetsa, 'Multi Objective Aerodynamic Shape Optimization of High Speed Train Nose Using Adaptive Surrogate Model'. Wright State University, Dayton, OH, 45435, USA, 2010
36. J. Muñoz-Paniagua , J. Garcia , A. Crespo and S. Krajnovic, Aerodynamic Optimization of the ICE 2 High-Speed Train Nose using a Genetic Algorithm and Metamodels, Eng. Ministry of Science and Technology, 2010

Appendices

Appendix I: Specification of ENT Passenger Car and Locomotive

1. Technical Specification for Electric Freight/ Passenger Locomotive 7200 KW AC

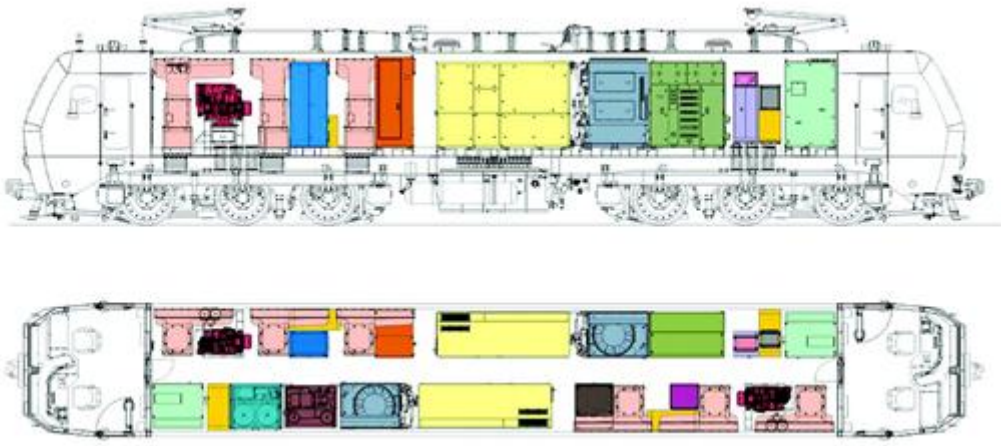

Figure AI0.1: HXD1C high power AC drive Six-axle (7200KW) Freight Electric

The following table shows some of the technical specifications ofHXD1C locomotive specification.

Table AI 0.1: HXD1C locomotive specification

No	Description	HDX1C specification
1	Load	5000t
2	Locomotive Weight	23t/25t
3	Auxiliary converter	248 KVA
4	Air brake	CCBII or EUROTROL
5	Electric brake	Regenerative
6	Car body	Compressive load 3000KN and tension load 2500KN in

		vertical direction
7	Axle load	23t or 25t
8	Axle type	CO-CO
9	Maximum operating speed	120 km/hr.

2. Technical Specification for Passenger Car: Technical Description of YZ25G Hard-seat Passenger Car

Table AI0.2 : Technical Specification for Passenger Car: Technical Description of YZ25G Hard-seat Passenger Car

No	Description	YZ25G specification	
1	General Technical Specification	Car strength	complies with TB/T1335-1996 《Railway vehicles Strength design and test evaluation specification》
		Vehicle dynamic performance	Complies with GB/T 5599-1985 《Railway Vehicle Dynamics Performance Evaluation and test identification norms》
		Vehicle gauge	complies with GB146.1-198 《Standard railway rolling stock gauge》
		Service life	30 years
		Maintenance period	Maintenance back to factory: 2.4 (±0.6)M Kilometers or 10years Maintenance in deport: 0.6(±20)M kilometers or 2.5years
		Conditions of Use	Maximum configuration: 20car per train set Ambient temperature: -40℃～+40℃ Maximum relative humidity ≤95%
		Platform height	Suitable for platform height with 300mm、500mm

			and1250mm, distance between platform edge and railway center is 1750mm
		Maximum line gradient	≤30‰
2	Main technical specification	Railway gauge	1435mm
		Maximum operation speed	120km/hr.
		Emergency brake distance	on straight line (with 30% overload and with initial speed 120km/h)≤800m
		Minimum negotiable curve	Single car 100m Coupling 145m
		Ride index	W≤2.5
		Noise (120Km/h)	≤68dB（A）
		Body static heat transfer coefficient (K)	≤1.16W/m2.k
		Illumination	Complies with TB/T2917－1998《Railway passenger coach illumination technical conditions》
		Axle load	≤17t
3	Main dimension	Car body length	25000mm
		Car body width	3105mm
		Height between rail top to car top(empty car)	4433mm
		Vehicle center distance	18000mm
		Height from rail top to coupler center (empty car)	880^{+10}_{-5} mm
		Height from rail top to	1333mm

		inter car crossing pedal (empty car)	
		Height from rail top to floor surface (empty car)	1283mm
		Car body center plate to rail top (empty car)	780mm
4	Car body steel structure	Body steel structure	Overall carrying beam cylindrical structure
		side wall	use flat plate
		Thickness of sheets and profiles	≤ 6mm will use nickel-chromium weathering steel, ≤ 2.5mm will use 05CuPCrNi, between 3 ~ 6mm will use 09CuPCrNi-B (Q295GNHL), Plate thickness more than 6mm will use ordinary carbon steel. Air conditioning seat, toilet and wash room iron floor whichever easily corrosive will use stainless steel.
5	Coupler and buffer device	Coupler	No.15 C-grade steel coupler, C-grade steel hook tail box
		Buffer	G1 buffer will be used.
6	Gangway and bridge plate	Gangway	Use rubber material
7	Bogie209P bogie	Construction speed	140km/hr.
		Axle	Axle load ≤17t, axle base: 2400mm
		Wheel	Overall rolling steel, diameter Φ915mm
		Damper	Proven hydraulic damper
		Bearing	NJ3226X1、NJP3226X1

		Axle box	Metal labyrinth seals, installed with digital sensor for axle temperature alarming
		Bogie safety performance	Derail parameter ≤1.0 Wheel load reduction rate ≤0.6 Overturning coefficient ≤0.8
8	Brake device		104 type air brake, Disk brake is used Handle brake will be set in car end one Emergency brake valve, brake pipe air pressure meter, main pressure meter will be installed on board. Brake on/release displayer will be set on both side of car body Brake pipe will use stainless material expect that on bogie which will use rubber.
9	Water supply and sanitation device	Water tank	Installed inside car, water can be supplied from both side of car body Use stainless material, volume≥1000 liters, water gauge is installed on every car.
		Toilet	Will use vacuum commode, two dirt collection boxes will be installed; volume of each will be not less than 550 liters.
10	Heating device(if needed)		Unit heating device with over-heat protection will be adopted, temperature and humidity control complies with GB/T12817
11	Air adjustment device		Roof mounted air condition will be used; temperature and humidity control complies with GB/T12817-2004. Toilet roof is set with nature ventilation.
12	Power supply and		DC600V

	illumination		Saloon lighting, toilet status displayer, axle heat warning device, electrical anti-slide device and communication deceive will use DC110V; tail light will use DC48V; AC socket will use AC220V; heating device will use DC600V; Air condition and water heater will use AC380V, control power will use DC110V. DC110V maintenance free alkaline battery will be used; capacity is not less than 120Ah. PLC electrical cabinet will be installed to supervise power supply, air condition, inverter, charger etc. DC110V online leakage detecting device will be set in PA power control box. Wire complies with LSZH requirement set in TB/T1484-2010 《locomotive cable》. Wiring complies with TB/T1759-2003 《 railway passenger coach wiring regulation》
13	Door, windows and interior eqmt.	Door	Folding doors will be used for car side and end, door panel will use weather resistance steel.
		Windows	Plastic sprayed aluminum window frame will be used
		Interior equipment	Each car will be set with 4 fire extinguishers. Each saloon will be set with 4 safety hammers, 1 in steward room. Rated Seat: 118 person

a. Interior layout drawing

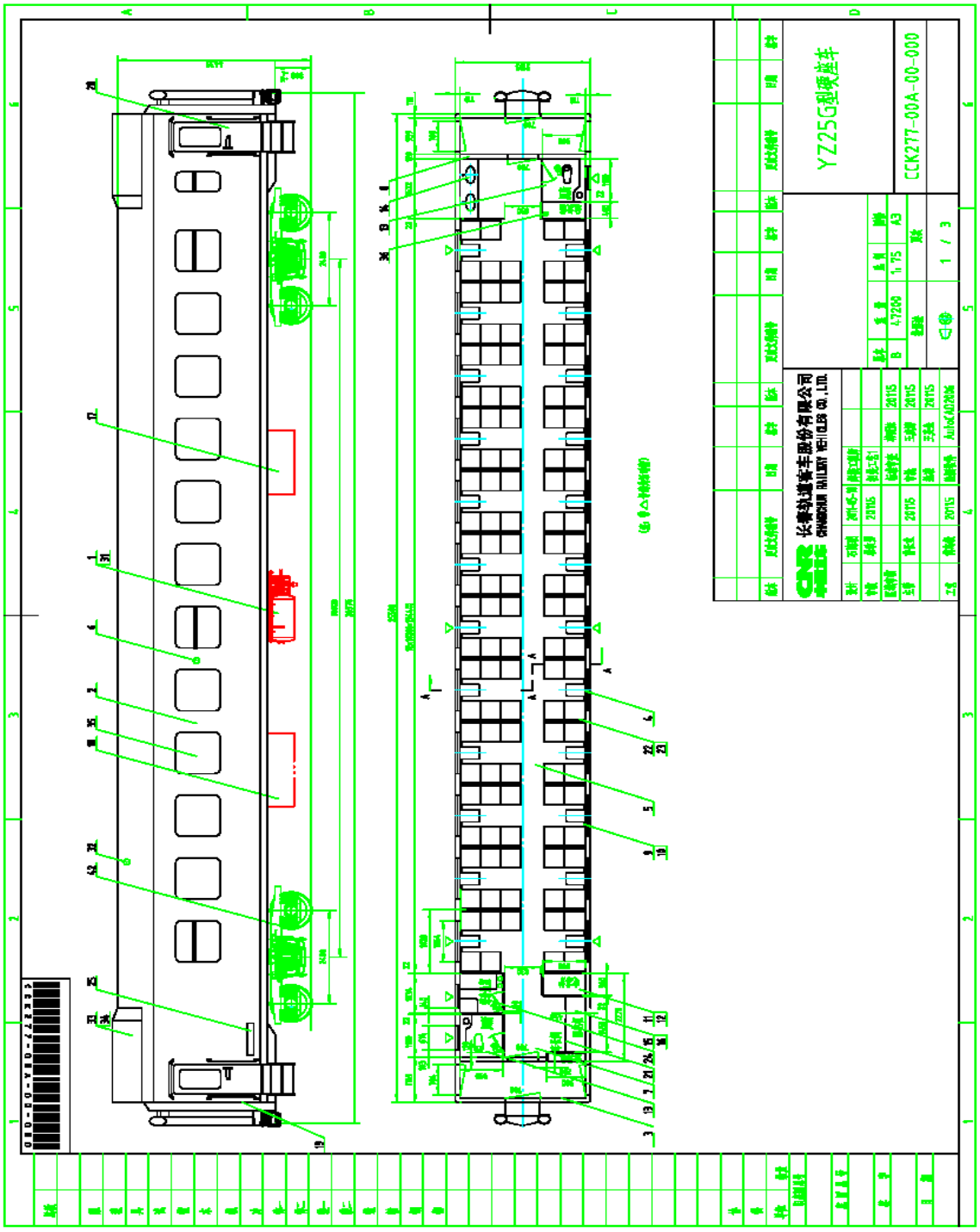

b. Car interior/exterior pictures

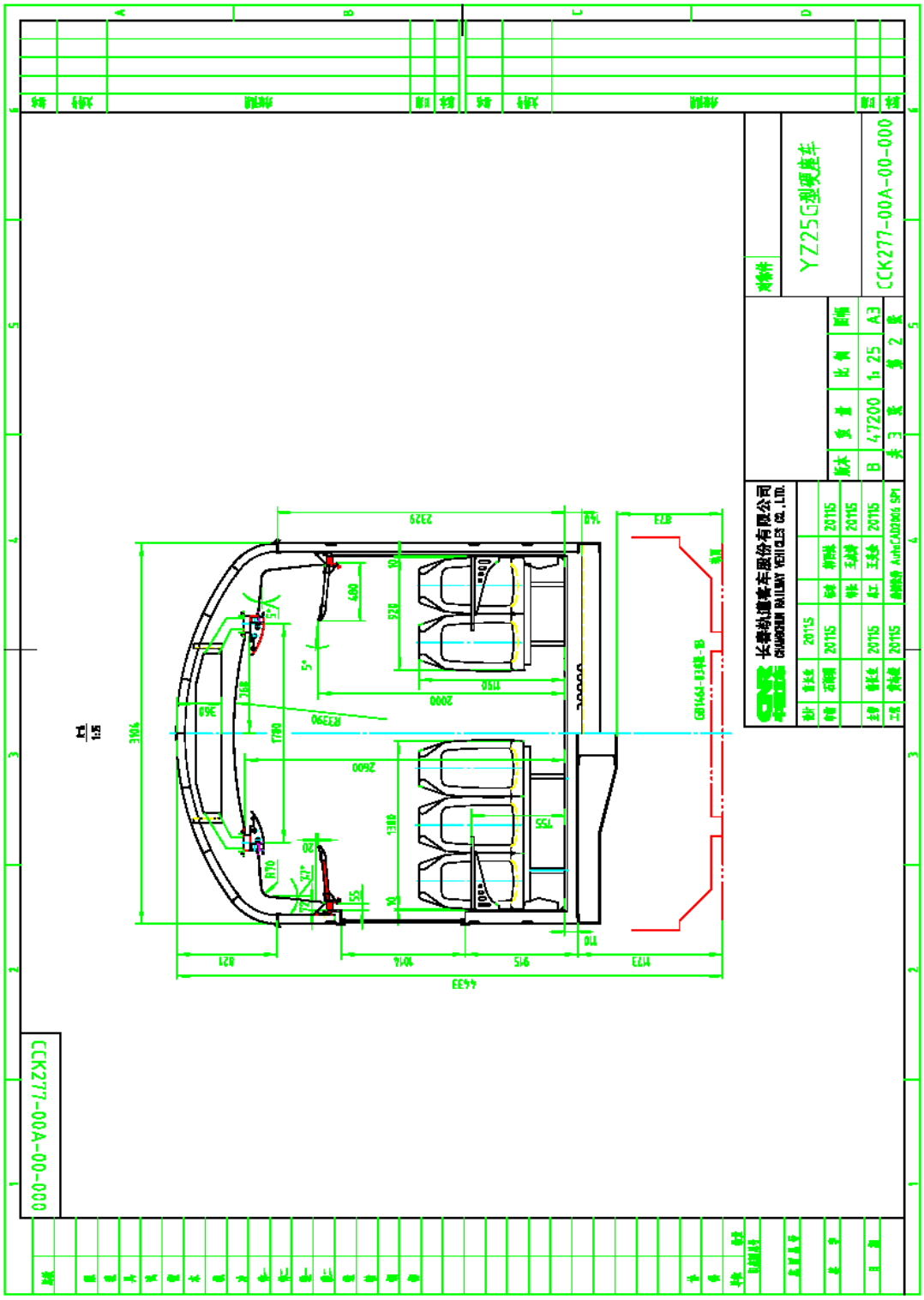

Figure AI0.2: Passenger car detailed drawings